CONTACT INFORMATION
Mining Records Curator
Arizona Geological Survey
1520 West Adams St.
Phoenix, AZ 85007
602-771-1601
http://www.azgs.az.gov
inquiries@azgs.az.gov

With the compliments of the authors.

Reprinted from:

PROCESS MINERALOGY VII-AS APPLIED TO
SEPARATION TECHNOLOGY, 1988

edited by:

A.H. Vassiliou, D.M. Hausen, and D.J. Carson

The Metallurgical Society
Warrendale, PA

Vivien Gornitz

ORIGIN OF THE ORPHAN MINE BRECCIA PIPE

URANIUM DEPOSIT, GRAND CANYON, ARIZONA

V. Gornitz,[1] K. J. Wenrich,[2] H. B. Sutphin,[2] and R. Vidale-Buden[3]

[1]Columbia University and NASA GSFC Institute for Space Studies, New York, N.Y. 10025
[2]U.S. Geological Survey, Denver, CO 80025
[3]University of New Mexico, Albuquerque, NM 87122

Abstract

The Orphan mine uranium deposit, Grand Canyon, Arizona, is a cylindrical collapse-breccia pipe, 70 to 150 m in diameter and 500 m deep. Pipe fill was derived from the Supai Group, Hermit Shale, and the Coconino Sandstone.

Uraninite, with Cu, Fe, Pb, Zn and Ni-Co sulfides is concentrated along the pipe boundary ring fracture (annular ring) and within the central porous sandstone matrix. There is some suggestion of vertical and lateral zonation of U with respect to Cu. Reduction of ferric oxide cement from red beds and recrystallization of carbonate, with formation of kaolinite preceded major ore deposition. Early Ni sulfides, arsenides and disseminated pyrite were followed by massive pyrite, and botryoidal uraninite, which in turn was succeeded by Cu, Zn and Pb sulfides. A second, later generation of uraninite was closely intergrown with hematite and base metal sulfides. Oxidation of primary minerals may have been associated with Tertiary regional uplift.

The paragenetic sequence closely resembles that of other Grand Canyon breccia pipes, except for the extensive development of the distinctive uraninite-hematite association. Mineral assemblages at the Orphan suggest possible mixing of the metal-bearing solution(s) with a more oxidized fluid, containing soluble uranyl complexes. Homogenization temperatures of fluid inclusions in calcite (60-110°C) at the Orphan fall within the lower end of the range observed at other breccia pipes.

Introduction

In the 1950s, less than a dozen Cu-U deposits in breccia pipes were known from the Grand Canyon area, among which was the Orphan mine uranium orebody. However, within the last decade, over 1000 additional collapse features have been discovered in northern Arizona, of which about 100 have been positively identified as collapse-breccia pipes. Half of these show surface indications of Cu minerals or anomalous γ-radiation, and several are currently being mined (Fig.1).

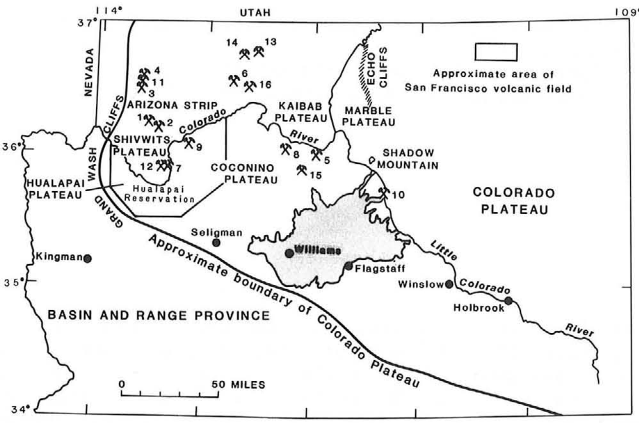

Figure 1. Index map of northern Arizona, showing the location of economic uranium deposits in breccia pipes. Numbers refer to the following mines:

1. Copper House	6. Hack Canyon	11. Savanic
2. Copper Mountain	7. Old Bonnie	12. Snyder
3. Cunningham	8. Orphan	13. Pigeon
4. Grand Gulch	9. Ridenour	14. Kanab North
5. Grandview	10. Riverview	15. Canyon

The Orphan Lode has been one of the most productive breccia pipe deposits, yielding four million lbs. of uranium oxide, seven million lbs. of copper and 107,000 oz. of silver (1). The Orphan mine site is located on an old mining claim, between Maricopa and Powell Points, about 2 1/2 miles west of Grand Canyon Village, Grand Canyon National Park, Coconino Co., Arizona. The claim was staked in 1893 and patented in 1906 for copper. Radioactivity was detected in 1951, and uranium production began in 1956. In 1962, legislation permitted the extension of mining underground beyond the boundaries of the original claim, in exchange for U.S. government title to the claim within 25 years. Mining ceased in 1969. The claim reverted to the Federal government in May, 1987.

The deposit lies in a nearly circular, vertical breccia pipe that crops out along the edge of the Grand Canyon, near the Coconino-Hermit Shale contact (Fig.2). The diameter of the pipe ranges between 220′ (67m) in the Hermit Shale, to 400′ (122m) within the Esplanade Sandstone, increasing to

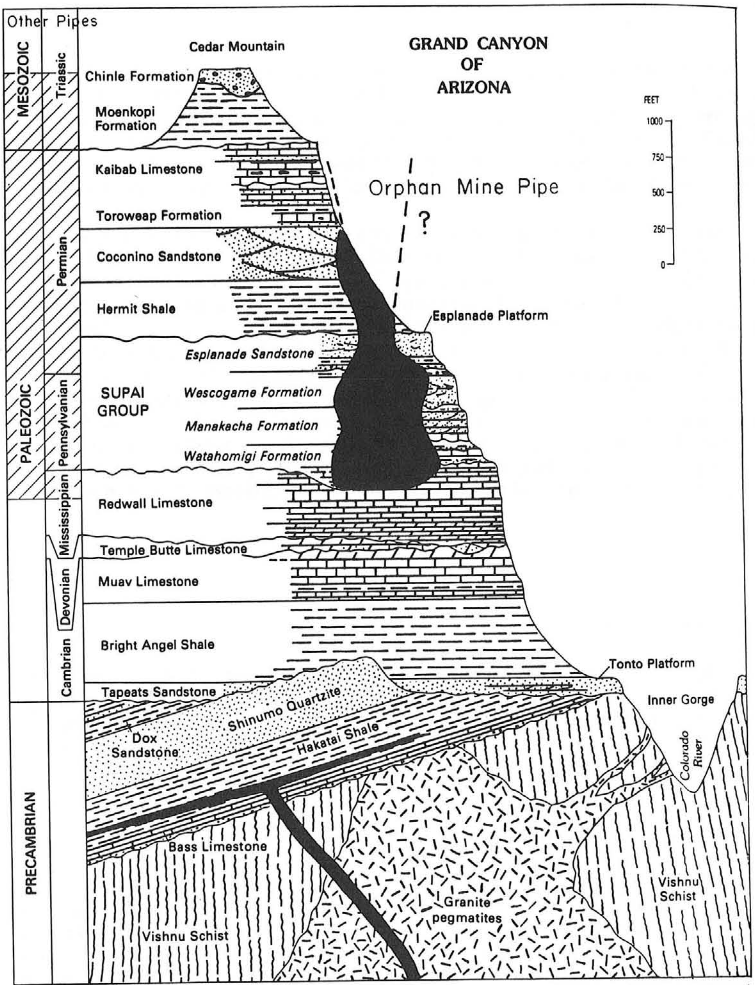

Figure 2. Stratigraphic section of the Grand Canyon, with the Orphan Pipe, and range of other breccia pipes.

over 500′ (152m) in the lower Supai Group. The pipe width is controlled to a large extent by wall rock lithology. The pipe boundary is defined by a set of concentric, circular tension fractures (the "annular ring"), which represent a favorable locus of ore deposition. According to Chenoweth (1), the stratigraphic range penetrated by the pipe extends from 300′ (91m) below the top of the Redwall Limestone to the Coconino Sandstone, a vertical extent of at least 1660′ (506m), see Fig.2. If the pipe formerly extended higher in the section, as is probable, the upper portions have been eroded by Grand Canyon dissection during the last 5 my.

The mineralogy and lithology of the pipe have been previously studied (2, 3, 4, 5). However, in this report the ore petrography, paragenesis, zoning, and geochemical setting of the Orphan are re-examined in light of an additional 15 years of breccia pipe exploration and research. Furthermore, the extensive data available for the Orphan orebody provides a basis of comparison with other newly discovered mineralized pipe structures.

Samples originally collected by the first author during field work in 1966 and 1967 were supplemented by additional material provided by W. Chenoweth (Grand Junction, Colo.) and from the U.S. Geological Survey archives. In this study, 29 sections were examined under the microscope in reflected light, and 40 in transmitted light, with magnifications up to 1000X. Because of the extremely fine-grained nature of many of the minor phases, the mineral paragenesis was established by microscopic analysis and interpretation of ore textures (6). Elemental x-ray maps for exceptionally fine-grained portions of several samples were obtained on an ARL electron microprobe, to identify fine mineral zonations. A tentative chemical model for the Orphan deposit has been outlined, based upon the paragenetic sequence of observed mineral assemblages, and published thermodynamic data.

Lithology

Unbrecciated host rocks

The Coconino Sandstone is a fine to medium-grained subrounded quartz sandstone (av. grain size 0.13 mm, >90% quartz, 2-3% microcline and plagioclase). The sandstone is cemented by quartz overgrowths and chert, with minor carbonate and limonite. A few larger, rounded quartz grains are present.

The Hermit Shale contains fine-grained subangular quartz (av. grain size, 0.06 mm, 15-45% quartz) coated by hematite and cemented by fine-grained dolomite. Minor amounts of feldspar and clay are present.

Samples from facies B of the lower Esplanade Sandstone (7) and from the upper Wescogame Formation of the Supai Group consist of well-sorted, very fine-grained, hematite-stained, calcareous sandstone (av. grain size 0.07 mm). The carbonate content is highly variable. The cement varies texturally from micritic calcite to a fine-grained mixture of anhedral calcite and euhedral rhombs of dolomite.

As one approaches the pipe along the 400 level crosscut, discontinuous bleached lenses appear several hundred feet southwest of the pipe contact. At this level, a circular bleached zone, approximately 30′-40′ (9-12m) wide, surrounds the margin of the pipe (Fig.3). A bleached zone of comparable width is also observed on the 245 level, in the Esplanade Sandstone. Petrographic examination of bleached samples shows reduction of hematite and recrystallization of calcareous cement to a coarser-grained calcite/dolomite mixture.

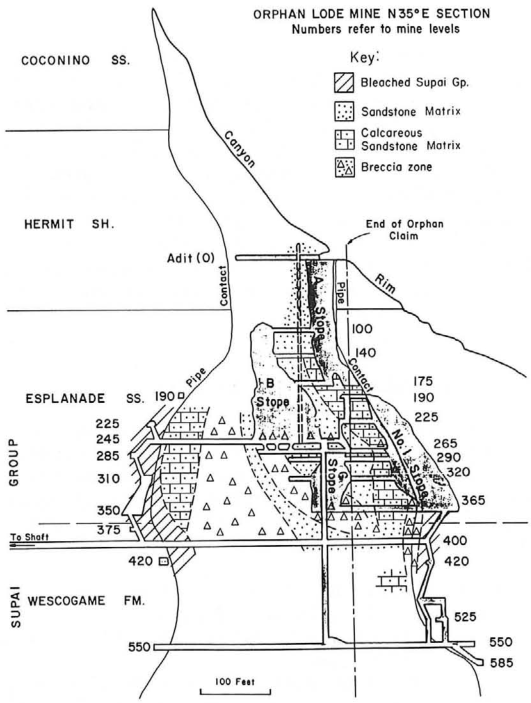

Figure 3. Cross-section of the Orphan breccia pipe, showing generalized geology.

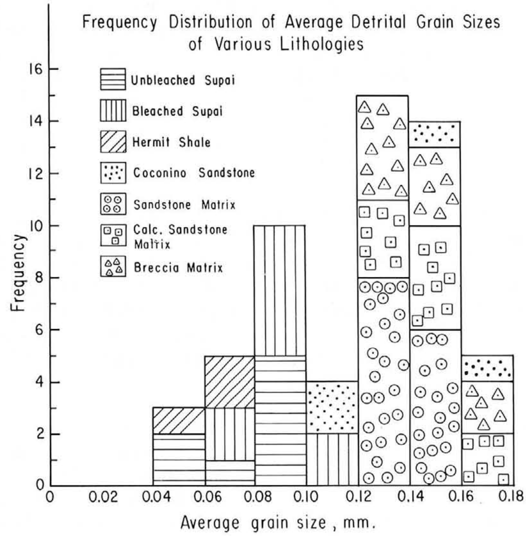

Figure 4. Histogram of average detrital grain diameters of samples from the Supai, Hermit and Coconino Formations, and pipe matrix sandstones.

Pipe breccia clasts

Breccia fragments range in size from a few millimeters to several meters. Lithologies include argillaceous, silty, micritic limestone, siltstone, dolomitic siltstone, shale and mudstone (see also Fig.3). Based on samples from the Bright Angel and Kaibab trails, plus literature descriptions (7,8), the breccia fragments can be traced largely to the Hermit Shale and Supai Group. Most pipe-fill sandstone occurs as breccia matrix, but large massive blocks of Coconino Sandstone have also been observed within the pipe (9). One fragment of oolitic, micritic limestone from the G stope, 365 level, could possibly have been derived from the Toroweap Formation. However, a similar-looking specimen was collected from the Supai Group, along the Kaibab Trail. Therefore, a Toroweap source for any of the breccia has not been determined with certainty.

Quartz sandstone and calcareous sandstone matrix

The breccia matrix consists of fine-grained subangular to subrounded quartz (>90%; average grain size 0.13 mm), with minor microcline and plagioclase. Near the pipe margins, the quartz content decreases and the matrix becomes more calcareous (up to 30-50% carbonate; average quartz grain size 0.14 mm; Fig.3). In parts of the pipe, much of the sandstone matrix is massive, with little or no breccia fragments (Fig.3).

Coconino quartz is readily distinguished from Supai or Hermit on the basis of average grain size distribution (Fig.4).

1) < 0.1 mm	Bleached and unbleached Supai, and Hermit Formations.
2) > 0.1 mm	Massive quartz and calcareous sandstone fill, breccia matrix, and Coconino Sandstone (from Grand Canyon trails).

The weighted average quartz grain size for the Supai samples examined in this report is 0.077 mm ±0.015 (N=17), that for pipe matrix is 0.14 mm ±0.013 (n=32), and that for the Coconino Sandstone (outside the pipe) is 0.13 ±0.03 (N=4). Comparison of the means, using the Student's T test, indicates that the average quartz grain sizes of the pipe matrix and Coconino samples are statistically identical, whereas the averages of matrix versus Supai (or Hermit) are significantly different at the 95% confidence level. These values do not support the Esplanade origin (1) for sandstone matrix, between the 75-450 levels.

Much of the Coconino sandstone appears to have been either weakly cemented or decemented at the time of collapse. Breccia fragments incorporated into bedded sandstone matrix probably resulted from filling of local cavities within the pipe by a slurry of loose sand and small rock fragments. Furthermore, Coconino quartz shows the greatest stratigraphic displacement among pipe fill materials, having been observed to the 430 level, or 630 ft (190m) below the Coconino-Hermit contact. This depth is a minimum estimate, as lower levels have not been sampled.

SiO_2 cementation of sandstone matrix may have occurred shortly after Coconino deposition, or later, after collapse of the loose quartz sand into the pipe. However, subsequent to collapse, carbonates filled the interstitial pore space within the matrix sand. Framework quartz grains are commonly unsupported and "float" in a coarse-grained (occasionally poikiolitic) calcite/ dolomite cement, which recrystallized from micritic calcite, relicts of which can still be seen in thin section. The open texture implies a high degree of porosity at the time of pipe-fill deposition.

The calcareous matrix cement may have been redeposited from carbonates dissolved from the upper Redwall Limestone, and lower Supai Group. Carbonate dissolution at depth would have provided space for the continuation of upward stoping. However, extensive dissolution of quartz and replacement by carbonates has not occurred at the mine levels under study, and thus massive quartz sandstone occurs intact in the pipe-fill (Fig. 3). Although, generally, calcite has only marginally corroded quartz along grain edges, some minor, localized occurrences of more thorough replacement have been noted.

Ore Mineralization and Paragenesis

Pre-ore alteration

That bleaching, or reduction of ferric oxides, probably preceded mineralization, is suggested by the enclosure of carbonate cement and ore minerals around the bleached materials. Hematitic haloes around uraninite (with associated sulfides) demonstrate a later iron-oxide overprint on already-bleached pipe-fill.

One may expect that the reduction of Fe^{+3} should produce an early generation of finely disseminated pyrite. This is supported by the presence of fine-grained cubic pyrite, evenly scattered in some breccia fragments, in contrast to coarser-grained subhedral to anhedral pyrite that replaced calcareous sandstone matrix. However, some of the observed textural differences of pyrite may have resulted from variations in porosity between clasts and matrix.

Recrystallization of carbonate cement in pipe fill also predated ore deposition, as the carbonates are a preferred site for massive ore replacement. The continued presence of dolomite in some heavily mineralized samples (e.g. 991-F-C85) suggests preferential replacement of calcite by ores. Crystallization of kaolinite into fibrous sheaves or rosettes may have been concurrent with or after carbonate recrystallization, since it commonly fills pore space between both quartz and calcite grains.

Early-stage mineralization

Barite was one of the first ore-related minerals to have formed after dolomite (Table I). Barite occurs as bladed or prismatic crystals, and as cement. Many of the larger barite crystals were replaced by pyrite and other sulfides. Barite was closely succeeded by siderite, which forms tiny clusters on both dolomite rhombs and barite blades. Although barite is predominantly an early phase, late-stage barite also occurs. For example, in sample 991-P-C86, barite has deposited after sulfides and uraninite.

Nickel/cobalt sulfides and arsenides also were deposited early in the sequence (Table I). Bravoite occurs as microscopic, brownish, isotropic cubes and octahedrons at the cores of pyrite cubes, and as thin bands in zoned pyrite (Fig.5). Much of the bravoite has decomposed or dissolved, leaving hollow casts. Siegenite also forms euhedral crystals in pyrite, or is enclosed by bravoite in pyrite. Gersdorffite appears in trace amounts in pyrite.

Nickel arsenides are less abundant, and occur in the annular ring. Nickeline (niccolite) is enclosed by rammelsbergite and pararammelsbergite. Rammelsbergite is euhedral, zoned, and has hollow cores that may have formed by dissolution of nickeline, in a manner analogous to the removal of bravoite within pyrite. These voids were partially filled later by bornite, digenite and covellite. An unidentified polymetallic sulfarsenide associated with rammelsbergite (Fig.6) was determined by microprobe analysis to contain Ni,

TABLE I. MINERAL PARAGENESIS OF THE ORPHAN MINE

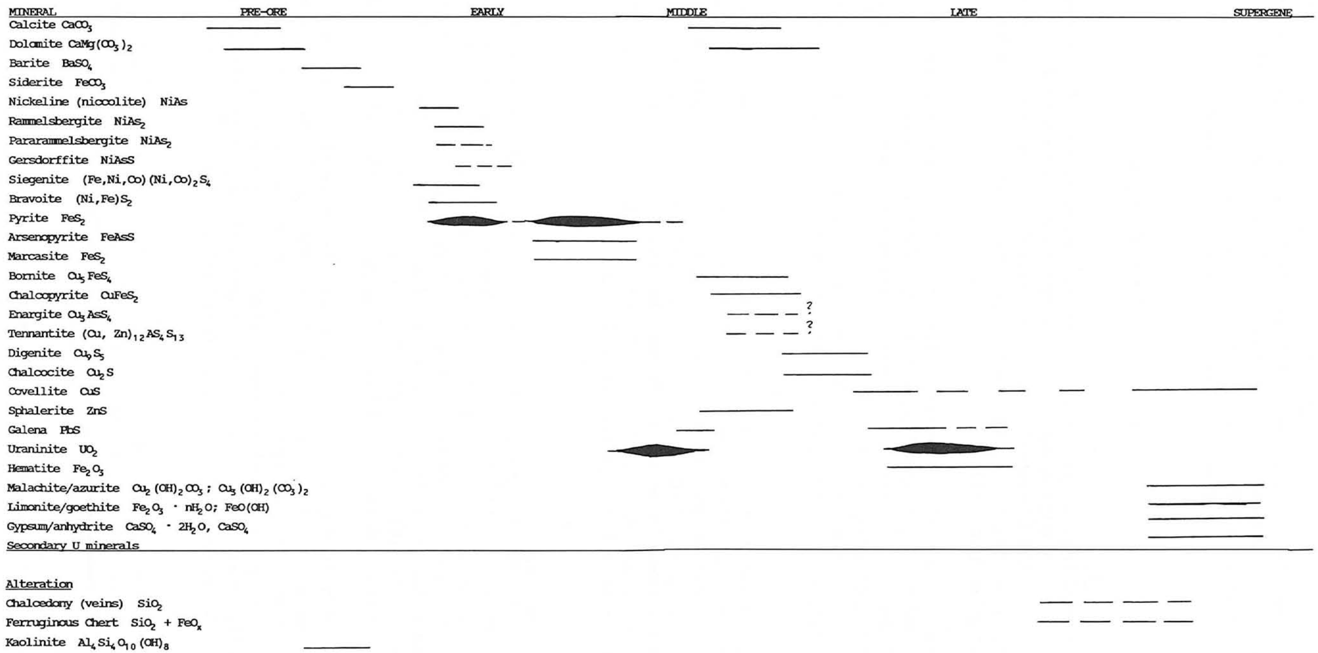

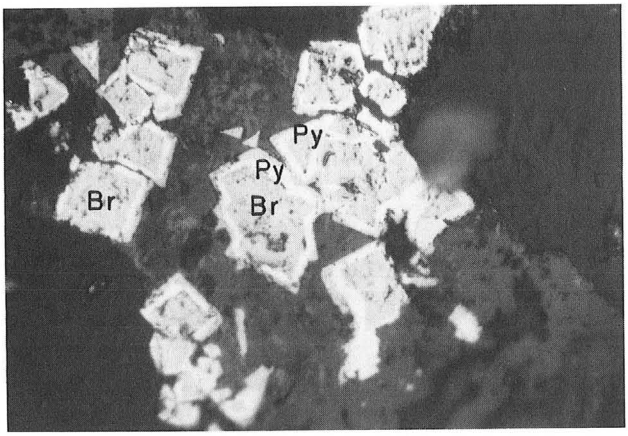

Figure 5. Zoned pyrite (Py) with bravoite cores (Br) (0.13 mm across).

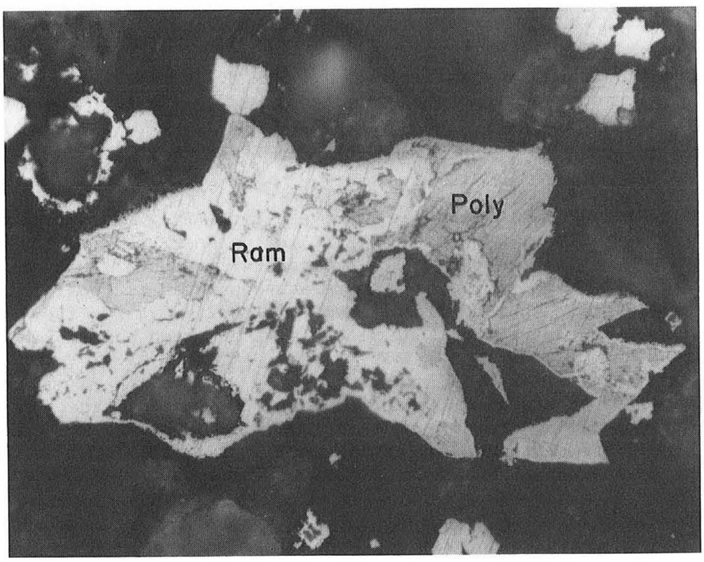

Figure 6. Rammelsbergite (Ram) with polymetallic phase (Poly), 420 level, annular ring (0.21 mm across).

Cu, with traces of Co and Zn. Other minute matrix crystals appear to be a mineral, as-yet unidentified, containing Cu, Zn, Ni, Co, S.

Pyrite is the most abundant sulfide mineral. Two discrete generations are present (Table 1). Early pyrite consists of very fine-grained, disseminated cubes, scattered interstitially between quartz grains, partly replacing cement, and cleavages of barite. This pyrite is strongly zoned, with cores and bands of bravoite and siegenite (Fig.5). Later, massive pyrite replaced carbonate cement within the pipe matrix, ultimately filling in cracks, and embaying quartz. A similar sequence is observed in sandstone deposits [Fig. 489 in (6)], and in other breccia pipes on the Colorado Plateau. Arsenopyrite and marcasite are usually found intergrown with massive pyrite.

Much of the massive pyrite is highly fractured. The fractures are filled with copper minerals such as digenite, chalcocite (Fig.7), and bornite as well as quartz and galena. Although fracturing could conceivably be linked to ore-related deformation and ore deposition, pyrite is the only sulfide which is strongly shattered. This may reflect the relative brittleness of pyrite, or crystallization pressure, due to emplacement of other ore minerals. For example, in several samples, intact detrital quartz grains are observed adjacent to fractured pyrite (e.g. sample no.1090/5630).

<u>Middle-stage mineralization</u>

Uraninite is the only primary uranium mineral. It forms thin coatings around quartz grains, less frequently, spherical or botryoidal masses (Fig.8), and in one sample from the 100 level, replaced silicified wood.

A very dark gray, isotropic phase occasionally appears as blebs or oriented blades along incipient shrinkage cracks in uraninite. Although microprobe analyses indicate that this dark phase is chemically identical with ordinary uraninite, it could be slightly more oxidized [p.1050 in (6)].

Botryoidal uraninite with shrinkage cracks filled by bornite and chalcopyrite clearly preceded these copper minerals (Fig.8). Due to inaccessibility of portions of the mine during field work as well as prior mining of high grade ore, it was not possible to determine the extent of early stage uraninite.

Copper minerals have succeeded massive pyrite (Fig.7,9) and early uraninite (Fig.8, Table I). Ragged pyrite inclusions remain in chalcopyrite, and bornite. Digenite and chalcocite are generally younger than either chalcopyrite or bornite. However, the relative paragenetic position of chalcopyrite vs. bornite, and digenite vs. chalcocite, varies from one section to another, suggesting that minerals within each pair formed more or less contemporaneously.

Chalcopyrite occurs as disseminated grains, oriented blades along (100) cleavage directions in bornite, and rims around bornite (Fig.8). The oriented blades are surrounded by a thin band of digenite. The relative proportions of chalcopyrite-bornite-digenite vary widely from grain to grain, less than several millimeters apart. In many grains the proportion of chalcopyrite to bornite is too great to be accounted for by exsolution. Therefore, these textures suggest replacement rather than exsolution.

Bornite commonly occurs in association with the other copper minerals. Tiny white blebs, identified as galena by microprobe analyses, occasionally appear in bornite (Fig.8). This galena may be older than the coarser grained galena found elsewhere.

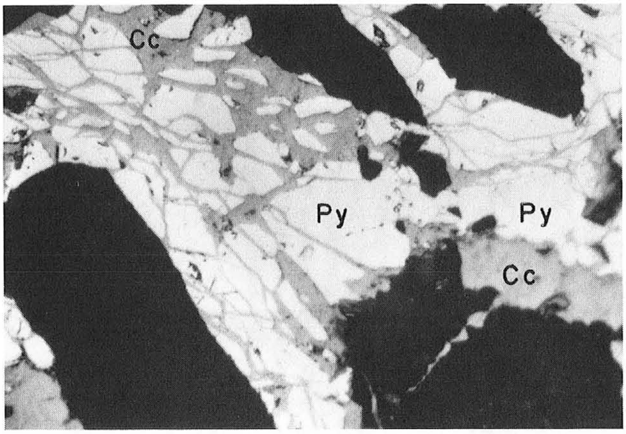

Figure 7. Highly fractured, massive pyrite (Py). Fractures are filled with chalcocite (Cc), 225 level (0.13 mm across).

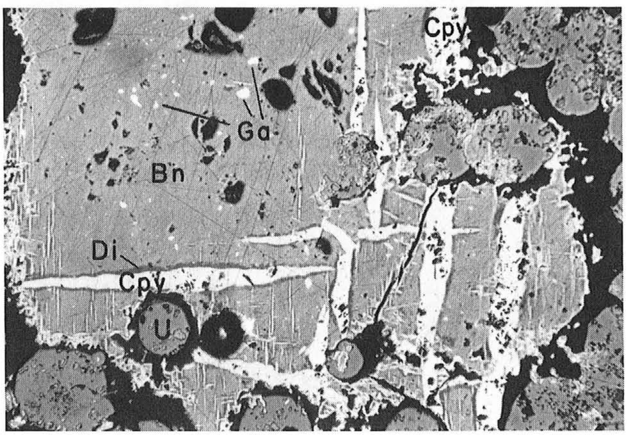

Figure 8. Botryoidal uraninite (U), with oriental blades of chalcopyrite (Cpy) and digenite (Di) in Bornite (Bn) in shrinkage cracks. Tiny blebs are galena (Ga), 420 level (0.45 mm across).

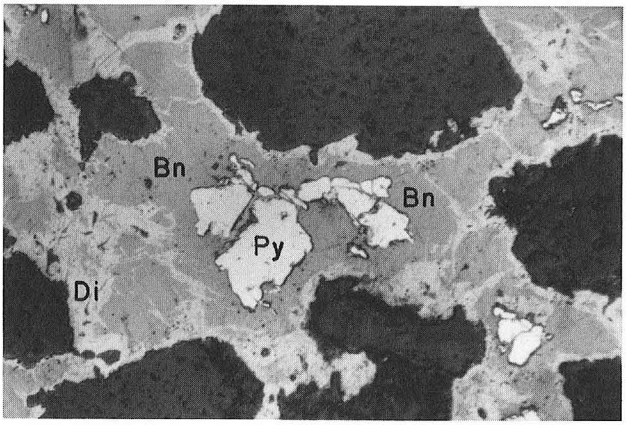

Figure 9. Pyrite (Py) remnants rimmed successively by bornite (Bn) and digenite (Di) (Thin section is 0.22 mm across).

Zn-bearing tennantite (identified by x-ray mapping on the electron microprobe) and enargite appear in trace amounts with the other copper minerals. Covellite replaces all other copper minerals, and is therefore the youngest copper sulfide.

Some carbonatization accompanied copper deposition. Digenite associated with dolomite is surrounded by later chalcocite (sample #11). Furthermore, large zoned calcite crystals, containing chalcopyrite inclusions, have been found (4).

Late-stage mineralization

That galena usually contains inclusions of pyrite, chalcopyrite, and sphalerite, but not the reverse, implies that galena crystallized after these minerals. The relative position of sphalerite is uncertain, but it is usually intergrown with galena and also contains inclusions of chalcopyrite.

A later stage of uraninite rims galena or copper sulfides indicating that it usually deposited after these minerals (Table I). However in some samples, galena appears to be younger than uraninite. The relatively late deposition of uraninite resembles the sequence observed at other mineralized Grand Canyon breccia pipes. Late-stage uraninite from the annular ring is often intergrown with base metal sulfides, nickel arsenides and hematite. These minerals tend to occur in discrete zones (Table II).

Table II. Summary of zonation in uraninite-hematite samples

	Hematite zone	bleached	transitional	uraninite zone
early				Ni sulfides and arsenides
	pyrite (rare)			pyrite
			bornite	bornite
	chalcopyrite	chalcopyrite (rare)	chalcopyrite	chalcopyrite
	digenite	digenite	digenite	chalcocite
	covellite		covellite	
	sphalerite (rare)			sphalerite
	galena (rare)			galena
	hematite			uraninite
late				(galena)

Supergene enrichment and secondary minerals

Secondary enrichment and oxidation may be related to the late Tertiary period of active dissection of the sediments (10). Some supergene enrichment of copper is suggested by the occurrence of chalcocite overlying chalcopyrite in the pipe (1), and replacement of other copper minerals by covellite. Partial oxidation of uraninite is also indicated by relatively small unit cell constants, suggesting a formula close to $UO_{2.34}$ (4). Fracture fillings of secondary minerals (e.g. malachite, gypsum, chalcedony), vugs of anhydrite or gypsum, and the diverse array of oxidized secondary minerals (3, 5) are probably associated with this episode.

Mineral Zonation

Uranium ore has accumulated in the annular ring, around the circumference of the pipe, as well as within the pipe. The distribution of ore within the pipe has been controlled by a combination of intrinsic lithological permeability and induced permeability through fracturing. Massive ore has preferentially accumulated in relatively porous sandstone pipe-fill, and calcareous sandstone matrix, and in more porous units within the Esplanade Sandstone adjacent to the pipe, relative to siltstone or shale breccia fragments. However, the last commonly contain fine-grained disseminated pyrite.

The location of stopes indicates that uraninite was deposited in economic grade quantities above the 365 level; the grade increased upward as the amount of associated galena increased. The highest grade uraninite was confined between the 225 level and the adit (0 level), in porous sandstone breccia matrix. The A stope at the stratigraphic level of the upper Esplanade Sandstone, above the 175 level, has yielded the highest grade ore (>1.5% U_3O_8), although rich ore also has been recovered from the center of the pipe (B and G stopes, Fig.3), and from the heavily brecciated northern pipe rim (No. 1 stope). Little commercial-grade ore was found below the 400 level, in the Wescogame Formation (Fig. 10).

Pyrite is disseminated throughout the vertical extent of the pipe. Uraninite, massive pyrite, and minor quantities of galena, sphalerite, arsenopyrite and marcasite have concentrated within the center of the pipe. Annular ring ore consists of a complex, very fine-grained assemblage of chalcopyrite, copper sulfides and nickel (cobalt) arsenides with uraninite and hematite (Fig. 10).

Copper mineralization accumulated to a greater extent below uranium between the 225 and 400 levels, than elsewhere in the pipe (Fig. 10). Chenoweth (1) found that copper minerals have concentrated in a lower-grade U ore zone, inside the higher-grade uranium ore zone of the annular ring. This pattern was best developed between the 225-350 levels. Chalcocite was more abundant than chalcopyrite on the upper levels of the annular ring (190-225 levels), whereas chalcopyrite became more prevalent between the 245-350 levels (1). However, the limited samples available in this study are insufficient to reconfirm the chalcocite-chalcopyrite zonation. The concentration of chalcocite above chalcopyrite would be consistent with some supergene enrichment. Not unexpectedly, oxidation has been more pronounced at the uppermost mine levels (1).

Nickel arsenides occur between the 400 and 420 levels, along the annular ring, on the north margin of the pipe. Barite and siderite are common within the northeastern half of the pipe (Fig. 10).

Geochemical Considerations

Bleaching

As mentioned above, hematite has been removed from red beds within and close to the Orphan breccia pipe, probably at an early stage, that preceded ore formation and long before the later stage of hematite associated with uraninite. A similar bleached (reduced) zone is observed in other breccia pipes, whether mineralized or not. This may suggest an independent, regional process although it is possible that bleached, unmineralized pipes have been mineralized in the past, but ore minerals have subsequently been removed by weathering or oxidation.

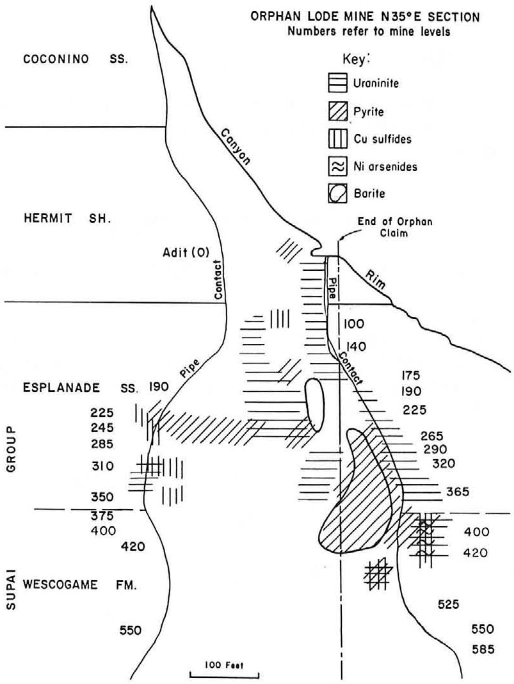

Figure 10. Cross-section of the Orphan breccia pipe, showing a schematic distribution of ore minerals.

The most likely reducing agents are organic compounds or H_2S. Only minor organic material is observed in the Orphan, mostly in plant fossils from the Hermit Shale and Esplanade Sandstone. Reduction of Fe^{+3} by H_2S is, therefore, more probable. A wide range of negative δ S^{34} values suggests a sedimentary or bacterial origin for the sulfur (5). Bleaching by H_2S-bearing fluid and the precipitation of the early, finely-disseminated pyrite can be expressed by reactions such as:

$$Fe_2O_3 + 2\ H_2S + 2H^+ = FeS_2 + Fe^{+2} + 2H_2O \qquad (1)$$

Middle Stage Mineralization

Uranyl complexes carried by an oxidizing solution (11) may have been reduced by H_2S, pyrite, or other early sulfides and arsenides to form massive uraninite. For example:

$$4UO_2(CO_3)^0 + H_2S + 4H_2O = 4UO_2 + 4H_2CO_3 + H_2SO_4 \qquad (2)$$

$$FeS_2 + 7UO_2(CO_3)^0 + 8H_2O = 7UO_2 + 7H_2CO_3 + Fe^{+2} + 2HSO_4^- \qquad (3)$$

Cu sulfides appear next in the sequence. If Cu were carried as cuprous complexes (12), oxidation would have been required to form many of the observed ore minerals, perhaps by mixing of a base metal-bearing fluid with a more oxidizing solution. For example:

$$10Cu(HS)_3^{-2} + 2Fe^{+2} + \tfrac{1}{2}2O_2 = 2Cu_5FeS_4 + H_2O + 6H_2S + 16HS^- \qquad (4)$$

$$2Cu(HS)_3^{-2} + 2Fe^{+2} + \tfrac{1}{2}O_2 = 2CuFeS_2 + H_2O + 2H_2S \qquad (5)$$

$$18Cu(HS)_3^{-2} + \tfrac{1}{2}2O_2 = 2Cu_9S_5 + H_2O + 8H_2S + 36HS^- \qquad (6)$$

$$2Cu(HS)_3^{-2} + \tfrac{1}{2}O_2 = 2CuS + H_2O + 4HS^- \qquad (7)$$

Late Stage Mineralization

A second period of uranium deposition is characterized by the distinctive hematite-uraninite-base metal sulfide zonation discussed above (Table II). A plot of mineral stability fields as a function of log fO_2 vs. log fS_2, at 100°C, for a number of common-base metal oxides and sulfides (Fig.11), provides useful insights into the nature of the late stage hematite-uraninite zonation. The resultant stability fields shown in Fig.11 are compatible with observed mineral phases, and provide an overview of the probable ranges of oxygen and sulfur fugacities. However, because of data limitations, the time-variations in fO_2 and fS_2 levels have not been modelled here.

In Figure 11, the boundary between hematite and pyrite is defined by a diagonal line from the Py-Mt-Hm triple point, lower left, going to the upper right. The observed mineral zonation crosses this line. The concentration of chalcopyrite near the contact between hematite and bleached zones (Table II) is consistent with the location of its wedge-shaped stability field, on both sides of the hematite-pyrite boundary. The convergence of the fields for the other observed copper and nickel minerals into a fairly small area suggests deposition under a limited fS_2 gradient.

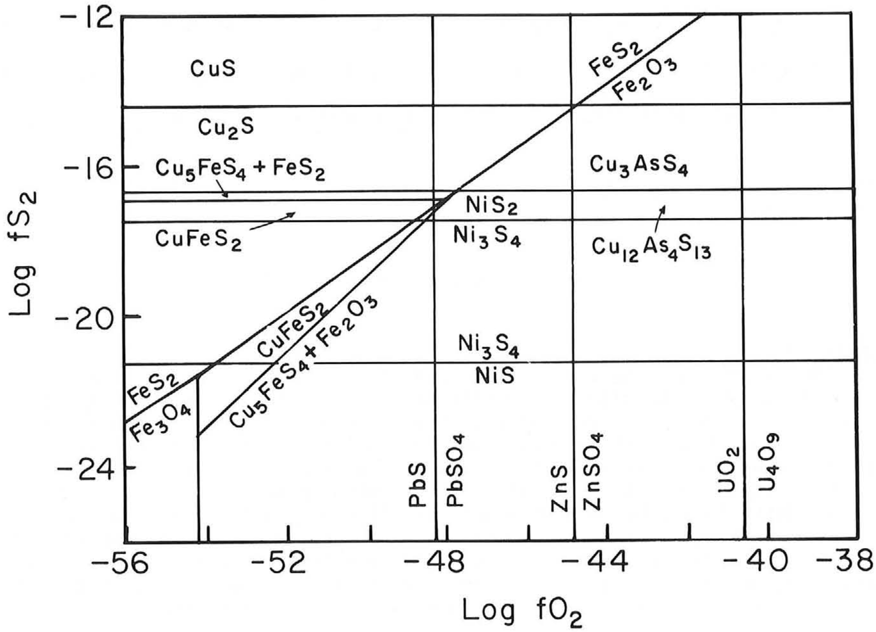

Figure 11. Mineral stability fields as a function of log fO_2 vs. log fS_2, at 100°C, for a number of common base-metal oxides and sulfides. The plotted minerals include hematite (Fe_2O_3), bornite (Cu_5FeS_4), chalcopyrite ($CuFeS_2$), pyrite (FeS_2), chalcocite (Cu_2S), covellite (CuS), galena (PbS), sphalerite (ZnS), uraninite (UO_2), U_4O_9, enargite (Cu_3AsS_4), vaesite (NiS_2), millerite (NiS), polydynite (Ni_3S_4), tennantite ($Cu_{12}As_4S_{13}$), anglesite ($PbSO_4$), and magnetite, Fe_3O_4.

The exact position of uraninite is determined by the stability of the uranyl complex, predominantly $UO_2(CO_3)^0$ at ~100°C (11). However, the univarient curve for the solid transition UO_2 - U_4O_9 is plotted instead, because of the availability of good thermodynamic data. The transition from UO_2 to uranyl complex plots well to the left of that line. Since uraninite and hematite do not co-exist in the zoned samples, and chalcopyrite has deposited <u>before</u> uraninite (Tables I, II), precipitation may have occurred under increasing fO_2 levels. The geometry of the mineral zonation therefore can be represented by a gradient in fO_2, higher at the hematite end, decreasing toward chalcopyrite, then uraninite, pyrite and nickel minerals. Some characteristic reactions may have been:

$$7UO_2(CO_3)^0 + FeS_2 + 8H_2O = 7UO_2 + Fe^{+2} + 2SO_4^{-2} + 7H_2CO_3 + 2H^+ \quad (8)$$

$$6UO_2(CO_3)^0 + NiAs_2 + 8H_2O = 6UO_2 + Ni^{+2} + 2AsO_4^{-3} + 6H_2CO_3 + 4H^+ \quad (9)$$

$$8UO_2(CO_3)^0 + CuFeS_2 + 8H_2O = 8UO_2 + Cu^{+2} + Fe^{++} + 8H_2CO_3 + 2SO_4^{-2} \quad (10)$$

$$4UO_2(CO_3)^0 + PbS + 4H_2O = 4UO_2 + Pb^{+2} + SO_4^{-2} + 4H_2CO_3 \quad (11)$$

Slightly further away, where the entering pore solutions retained a higher oxygen fugacity:

$$2Fe^{+2} + \tfrac{1}{2}O_2 + H_2O = Fe_2O_3 + 4H^+ \quad (12)$$

<u>Mineralizing Fluids</u>

The early bleaching suggests the passage of sulfide-bearing fluids early in the history of the pipes. The base metals (Cu, Ni, Pb, and Zn) may have also been transported by sulfide-rich fluids at a later time, although their total solubility in such solutions may be too low (11, 13). Alternately, they may have been carried by NaCl-rich brines, such as observed in fluid inclusions (14, 15). However, transport of uranium requires a different, more oxidized fluid, because uranium is sufficiently soluble only as uranyl (U^{+6}) complexes (11). The existence of sulfate for barite formation and the formation of later hematite also requires a more oxidizing fluid. Thus, at least two, and probably more different transporting fluids were necessary for the formation of mineral assemblages observed in the Orphan pipe.

The concept of combining different fluids within these pipes is quite plausible. The pipe structure would facilitate the mixing of solutions derived from different rock strata, in a way analogous to the intersection of permeable zones by a drill hole. The chemistry and flow rate of the solutions entering the pipe could vary significantly through geologic time.

<u>Comparison of the Orphan Pipe with Other Grand Canyon Breccia Pipes</u>

Breccia pipes and associated orebodies are remarkably similar throughout the Grand Canyon region, an area covering almost one-fourth of the state of Arizona. The diameters of all of the known breccia pipes fall within a narrow range of about 30 to 150 m. The grade and tonnage of the ore within the Orphan Mine is comparable to other pipes presently being mined, although the ore at the Orphan seems to have been more concentrated around the annular ring, whereas at other mines, the bulk of the ore occurs within the pipe.

Perhaps the most striking similarity lies in the paragenesis. The repeated recurrence of the same extensive suite of minerals at the Orphan and other pipes cannot be mere coincidence. The paragenetic sequence established here for the Orphan varies only slightly from that observed in other breccia pipe orebodies. In fact, the crystallization sequence is almost identical; the difference lies more with the percentage of each mineral phase deposited at a specific time in the paragenetic sequence of each pipe.

Some of the major similarities, and a few differences are summarized below: (1) U-Pb dating establishes a narrow period of U mineralization for the Grand Canyon pipes [between 220-200 ma (16)]. (2) The Orphan mine clearly contains an early phase of botryoidal uraninite. This was not originally observed in other pipes, but a careful check has shown that at least one of the other mines also was found to contain minor amounts of this early botryoidal uraninite. (3) The mottled hematite-uraninite banding associated with the late stage uraninite appears to be far more prevalent in the Orphan ore than in most other orebodies, although at least two of the other pipes have notable examples of such an association. (4) The final stage pyrobitumen that is densely concentrated in at least one pipe, and observed in several others, occurs only in trace amounts at the Orphan (1). (5) Early anhydrite associated with barite does not appear to be prevalent at the Orphan, as it is at several other pipes.

Temperatures of formation also show close affinities (17). Fluid inclusion studies of several pipes yield filling temperatures of 80-145°C in dolomite, quartz, and sphalerite, with high salinities averaging 15 wt % NaCl (14). At the Hack 1 and 2 mines, homogenization temperatures of fluid inclusions in sphalerite range from 93 to 115°C, and salinity between 9.9 and 16.4 wt % eq. NaCl (15). Temperatures of 70-80°C have been found for carbonates (18). Collectively, these temperatures are somewhat higher than the 60-110° from calcite (linked to copper stage mineralization) at the Orphan (5).

The stratigraphic level of the ore at the Orphan is somewhat lower than at most of the pipes on the north rim. Almost all of the ore from the Orphan came from the statigraphic level of the Esplanade Sandstone, although this could be in part attributed to the removal of the upper portions of the pipe by erosion. It is possible that ore had previously been concentrated in the upper Hermit or Coconino levels, but was subsequently removed by canyon downcutting. Nevertheless, many of the pipes on the north rim do not have ore extending down into the Esplanade Sandstone, and ore from one pipe that does only extends partially into the Esplanade. One other orebody on the south rim apparently has ore at the same lower horizon as the Orphan. These relationships suggest that, at the time of deposition, the Coconino and Hermit on the north rim were at lower topographic elevations in the basin, thereby permitting mineralization at a higher stratigraphic level.

This study was based on a relatively small number of samples. As more data become available from the opening of new mines, more similarities or disparities between pipes may become evident.

Conclusions

The Orphan breccia pipe formed by collapse of overlying sediments into a sinkhole or cavern within the upper Redwall Limestone, which initially developed 325 my ago (19). Petrographic study of pipe-fill and background samples collected along Grand Canyon trails establishes that the pipe-fill is derived from units within the Supai Group, Hermit Shale and Coconino Sandstone. Textural evidence suggests that the Coconino Sandstone was largely unconsolidated or decemented during collapse. The youngest pipe-fill material (in this case Coconino, since Toroweap or Kaibab units have not been positively identified) limits the upper age of the structure. Thus, the pipe could be as old as mid-Permian, well predating Triassic uranium mineralization (16). Alternatively, the Late Mississippian paleokarst may have been reactivated during the Triassic, under a monsoonal climate (20), which produced fluctuating water tables. Such hydrologic conditions would have promoted the formation of sinkholes (21), and would have facilitated further upward stoping.

The accumulation of uranium ore in the annular ring and within the pipe was strongly controlled by fracturing and permeability. High grade uranium ore concentrated above the 225 level, whereas copper mineralization accumulated below the 225 level. There is also some indication of lateral zonation of U and Cu along the annular ring zone (1). Annular ring ore consists of a complex assemblage of uraninite/hematite with base metal sulfides and arsenides. New phases detected in this study include Zn-tennantite and a multimetallic element phase associated with rammelsbergite.

The paragenetic sequence at the Orphan includes deposition of early Ni sulfides and arsenides, succeeded by two generations of pyrite: fine-grained cubes and massive pyrite. These early minerals were followed by botryoidal uraninite and later by chalcopyrite, bornite, spalerite, galena and copper sulfides. A later generation of uraninite may have precipitated by reactions with previously deposited sulfides, and reoxidation of ferrous iron at greater distances. The observed mineral paragenesis is consistent with mixing of at least two different solutions, enhanced by the permeable environment within the breccia pipe.

The paragenetic sequence of the Orphan is closely paralleled by other Grand Canyon breccia pipes. Homogenization temperatures of fluid inclusions also fall within the range observed at other pipes (5,15). Major differences are the near absence of bitumens or hydrocarbons and of early anhydrite at the Orphan.

Acknowledgments

The first author wishes to thank Drs. M. Prinz and M. Weissberg for permission to use the research ore microscope at the American Museum of Natural History, New York City. Discussions with Dr. G. Bowles (U.S. Geological Survey, Denver) and Dr. D. Pohl (American Museum of Natural History) have been very helpful. This study is part of a larger project on the breccia pipes of northern Arizona, funded by the Bureau of Indian Affairs, and the U.S. Geological Survey.

REFERENCES

1. W.L. Chenoweth, "The Orphan Lode Mine, Grand Canyon, Arizona, A Case History of a Mineralized, Collapse-Breccia Pipe" (U.S. Geol. Survey Open-file Report 86-510, 1986), 1-91.

2. M.E. Kofford, "The Orphan Ore Deposit" (Unpubl. Mine Report, 1956).

3. M.E. Kofford, "The Orphan Mine" in "Geology and Natural History of the Grand Canyon Region," Four Corners Geol. Soc. Fifth Field Conf., (1969), 180-194.

4. V.M. Gornitz, "Mineralization, Alteration and Mechanism of Emplacement, Orphan Ore Deposit, Grand Canyon, Arizona" (Ph.D. Dissertation, Columbia University, 1969).

5. V. Gornitz and P.F. Kerr, "Uranium Mineralization and Alteration, Orphan Mine, Grand Canyon, Arizona," Econ. Geol., 65 (1970), 751-768.

6. P. Ramdohr, The Ore Minerals and Their Intergrowths, vol. 2 (Oxford and New York: Pergamon Press, 1980), 1269 p.

7. E.D. McKee, "The Supai Group of Grand Canyon," U.S. Geol. Surv. Prof. Paper, 1173(1982), 1-504.

8. D. White, "Flora of the Hermit Shale, Grand Canyon, Arizona," Carnegie Inst. Washington, 405(1929), 1-221.

9. C.G. Bowles, private communication with author, U.S. Geological Survey, Denver, 24 February 1987.

10. C.G. Bowles, "Economic Implications of a New Hypothesis of Origin of Uranium and Copper-Bearing Breccia Pipes, Grand Canyon, Arizona," U.S. Geol. Surv. Circ., 753 (1977), 25-27.

11. D. Langmuir, "Uranium Solution-Mineral Equilibria at Low Temperatures with Applications to Sedimentary Ore Deposits," Mineral. Assoc. Canada Short Course in Uranium Deposits, ed. M.M. Kimberley (Toronto: U. Toronto Press, 1978), 17-55.

12. H.L. Barnes, "Solubilities of Ore Minerals," Geochemistry of Hydrothermal Ore Deposits, ed. H.L. Barnes (New York: Wiley-Interscience, 1979), 404-460.

13. H.L. Barnes, "Ore-Depositing Reactions in Mississippi Valley-Type Deposits," Proc. International Conf. on MVT Pb-Zn Deposits, eds. Kisvarsanyi et al. (Rolla, Mo: University of Missouri, 1983), 77-85.

14. K.J. Wenrich, and L.M. Pratt, "Paragenesis and Conditions of Formation of Ore Minerals from Metalliferous Breccia Pipes, N. Arizona," G.S.A. Abstr. and Prog., 17 (1985), 747.

15. J.D. Rasmussen, C.G. Cunningham, and A.M. Gautier, "Primary Fluid Inclusions in Sphalerite from the Hack 1 and 2 Mines, Mohave Co., Arizona," G.S.A. Abstr. and Prog., 18(5)(1986), 404.

16. K.R. Ludwig, J.D. Rasmussen, and K.R. Simmons, "Age of Uranium Ores in Collapse-Breccia Pipes in the Grand Canyon Area, Northern Arizona," G.S.A. Abstr. and Prog., 18 (1986), 392.

17. K.J. Wenrich, "Mineralization of Breccia Pipes in Northern Arizona," Econ. Geol., 80 (1985), 1722-1735.

18. P. Landais, "Geochemical Analysis of the Organic Matters Associated with the Breccia Pipes in the Grand Canyon Area," G.S.A. Abstr. and Prog., 18(5)(1986), 389.

19. G. Billingsley, "Relations of the Surprise Canyon and Watahomigi Formations to Breccia Pipes in the Grand Canyon, Arizona," G.S.A. Abstr. and Prog., 18(5)(1986), 342.

20. R. Dubiel, "Sedimentology of the Upper Triassic Chinle Formation, Southeastern Utah" (Ph.D. Dissertation, University of Colorado, 1987), 1-125.

21. B.F. Beck, R. Ceryak, D.T. Jenkins, T.M. Scott, and D.P. Spangler, "Karst Hydrogeology of Central and Northern Florida, Field Guidebook," (Report 85-86-1, G.S.A. Annual Meeting, Orlando, Florida, 1985).

1988 SCANNED NJN 2008

ORIGIN OF THE ORPHAN MINE BRECCIA PIPE

URANIUM DEPOSIT, GRAND CANYON, ARIZONA

V. Gornitz,[1] K. J. Wenrich,[2] H. B. Sutphin,[2] and R. Vidale-Buden[3]

[1]Columbia University and NASA GSFC Institute for Space Studies, New York, N.Y. 10025
[2]U.S. Geological Survey, Denver, CO 80025
[3]University of New Mexico, Albuquerque, NM 87122

Abstract

The Orphan mine uranium deposit, Grand Canyon, Arizona, is a cylindrical collapse-breccia pipe, 70 to 150 m in diameter and 500 m deep. Pipe fill was derived from the Supai Group, Hermit Shale, and the Coconino Sandstone.

Uraninite, with Cu, Fe, Pb, Zn and Ni-Co sulfides is concentrated along the pipe boundary ring fracture (annular ring) and within the central porous sandstone matrix. There is some suggestion of vertical and lateral zonation of U with respect to Cu. Reduction of ferric oxide cement from red beds and recrystallization of carbonate, with formation of kaolinite preceded major ore deposition. Early Ni sulfides, arsenides and disseminated pyrite were followed by massive pyrite, and botryoidal uraninite, which in turn was succeeded by Cu, Zn and Pb sulfides. A second, later generation of uraninite was closely intergrown with hematite and base metal sulfides. Oxidation of primary minerals may have been associated with Tertiary regional uplift.

The paragenetic sequence closely resembles that of other Grand Canyon breccia pipes, except for the extensive development of the distinctive uraninite-hematite association. Mineral assemblages at the Orphan suggest possible mixing of the metal-bearing solution(s) with a more oxidized fluid, containing soluble uranyl complexes. Homogenization temperatures of fluid inclusions in calcite (60-110°C) at the Orphan fall within the lower end of the range observed at other breccia pipes.

Introduction

In the 1950s, less than a dozen Cu-U deposits in breccia pipes were known from the Grand Canyon area, among which was the Orphan mine uranium orebody. However, within the last decade, over 1000 additional collapse features have been discovered in northern Arizona, of which about 100 have been positively identified as collapse-breccia pipes. Half of these show surface indications of Cu minerals or anomalous γ-radiation, and several are currently being mined (Fig.1).

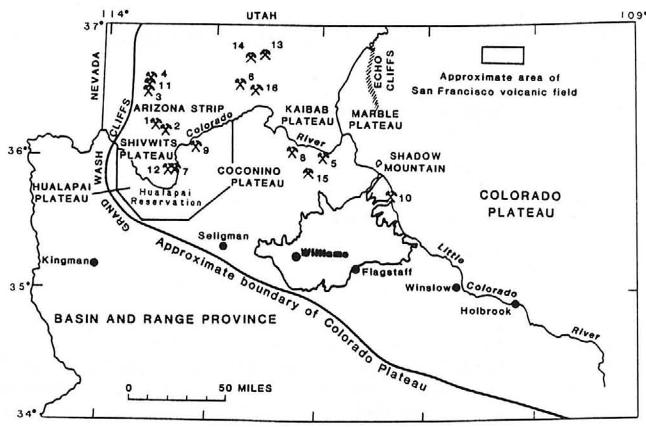

Figure 1. Index map of northern Arizona, showing the location of economic uranium deposits in breccia pipes. Numbers refer to the following mines:

1. Copper House
2. Copper Mountain
3. Cunningham
4. Grand Gulch
5. Grandview
6. Hack Canyon
7. Old Bonnie
8. Orphan
9. Ridenour
10. Riverview
11. Savanic
12. Snyder
13. Pigeon
14. Kanab North
15. Canyon

The Orphan Lode has been one of the most productive breccia pipe deposits, yielding four million lbs. of uranium oxide, seven million lbs. of copper and 107,000 oz. of silver (1). The Orphan mine site is located on an old mining claim, between Maricopa and Powell Points, about 2 1/2 miles west of Grand Canyon Village, Grand Canyon National Park, Coconino Co., Arizona. The claim was staked in 1893 and patented in 1906 for copper. Radioactivity was detected in 1951, and uranium production began in 1956. In 1962, legislation permitted the extension of mining underground beyond the boundaries of the original claim, in exchange for U.S. government title to the claim within 25 years. Mining ceased in 1969. The claim reverted to the Federal government in May, 1987.

The deposit lies in a nearly circular, vertical breccia pipe that crops out along the edge of the Grand Canyon, near the Coconino-Hermit Shale contact (Fig.2). The diameter of the pipe ranges between 220' (67m) in the Hermit Shale, to 400' (122m) within the Esplanade Sandstone, increasing to

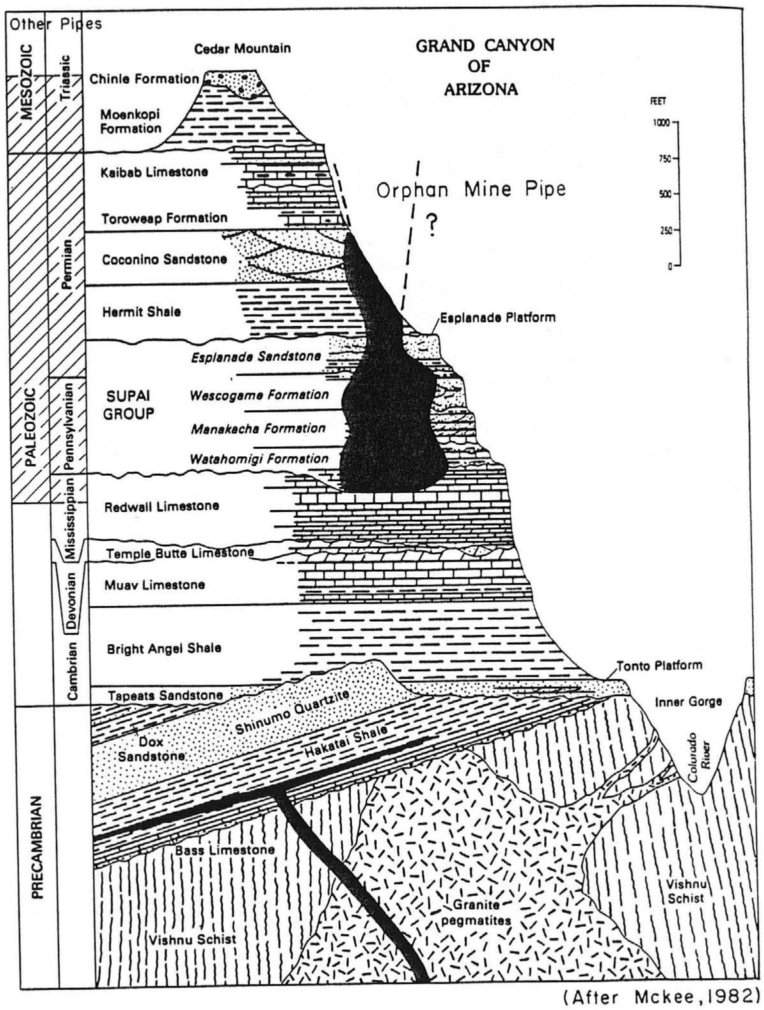

Figure 2. Stratigraphic section of the Grand Canyon, with the Orphan Pipe, and range of other breccia pipes.

over 500' (152m) in the lower Supai Group. The pipe width is controlled to a large extent by wall rock lithology. The pipe boundary is defined by a set of concentric, circular tension fractures (the "annular ring"), which represent a favorable locus of ore deposition. According to Chenoweth (1), the stratigraphic range penetrated by the pipe extends from 300' (91m) below the top of the Redwall Limestone to the Coconino Sandstone, a vertical extent of at least 1660' (506m), see Fig.2. If the pipe formerly extended higher in the section, as is probable, the upper portions have been eroded by Grand Canyon dissection during the last 5 my.

The mineralogy and lithology of the pipe have been previously studied (2, 3, 4, 5). However, in this report the ore petrography, paragenesis, zoning, and geochemical setting of the Orphan are re-examined in light of an additional 15 years of breccia pipe exploration and research. Furthermore, the extensive data available for the Orphan orebody provides a basis of comparison with other newly discovered mineralized pipe structures.

Samples originally collected by the first author during field work in 1966 and 1967 were supplemented by additional material provided by W. Chenoweth (Grand Junction, Colo.) and from the U.S. Geological Survey archives. In this study, 29 sections were examined under the microscope in reflected light, and 40 in transmitted light, with magnifications up to 1000X. Because of the extremely fine-grained nature of many of the minor phases, the mineral paragenesis was established by microscopic analysis and interpretation of ore textures (6). Elemental x-ray maps for exceptionally fine-grained portions of several samples were obtained on an ARL electron microprobe, to identify fine mineral zonations. A tentative chemical model for the Orphan deposit has been outlined, based upon the paragenetic sequence of observed mineral assemblages, and published thermodynamic data.

Lithology

Unbrecciated host rocks

The Coconino Sandstone is a fine to medium-grained subrounded quartz sandstone (av. grain size 0.13 mm, >90% quartz, 2-3% microcline and plagioclase). The sandstone is cemented by quartz overgrowths and chert, with minor carbonate and limonite. A few larger, rounded quartz grains are present.

The Hermit Shale contains fine-grained subangular quartz (av. grain size, 0.06 mm, 15-45% quartz) coated by hematite and cemented by fine-grained dolomite. Minor amounts of feldspar and clay are present.

Samples from facies B of the lower Esplanade Sandstone (7) and from the upper Wescogame Formation of the Supai Group consist of well-sorted, very fine-grained, hematite-stained, calcareous sandstone (av. grain size 0.07 mm). The carbonate content is highly variable. The cement varies texturally from micritic calcite to a fine-grained mixture of anhedral calcite and euhedral rhombs of dolomite.

As one approaches the pipe along the 400 level crosscut, discontinuous bleached lenses appear several hundred feet southwest of the pipe contact. At this level, a circular bleached zone, approximately 30'-40' (9-12m) wide, surrounds the margin of the pipe (Fig.3). A bleached zone of comparable width is also observed on the 245 level, in the Esplanade Sandstone. Petrographic examination of bleached samples shows reduction of hematite and recrystallization of calcareous cement to a coarser-grained calcite/dolomite mixture.

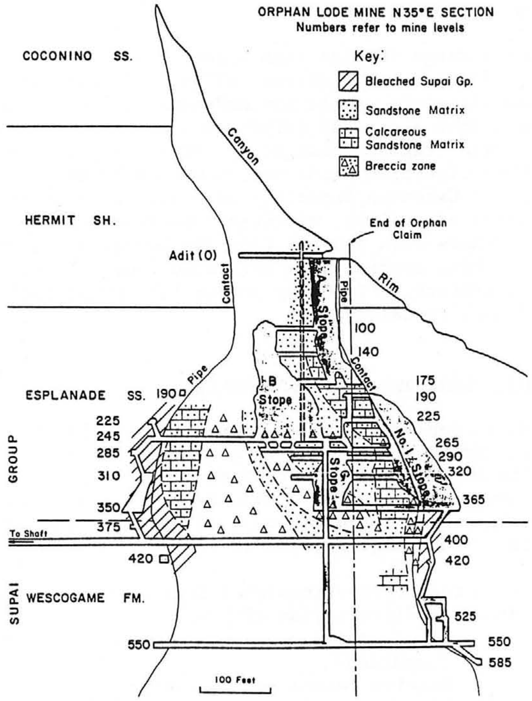

Figure 3. Cross-section of the Orphan breccia pipe, showing generalized geology.

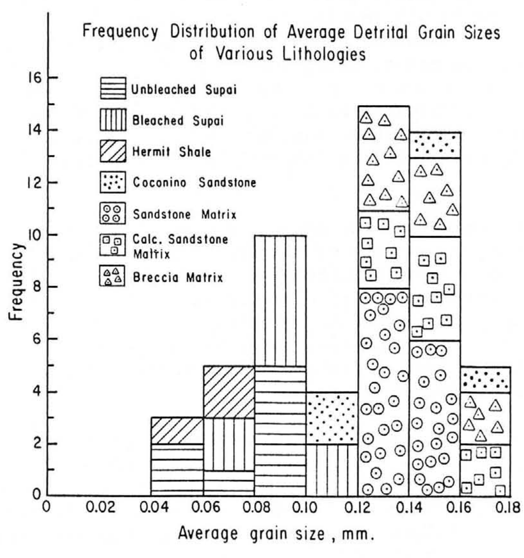

Figure 4. Histogram of average detrital grain diameters of samples from the Supai, Hermit and Coconino Formations, and pipe matrix sandstones.

Pipe breccia clasts

Breccia fragments range in size from a few millimeters to several meters. Lithologies include argillaceous, silty, micritic limestone, siltstone, dolomitic siltstone, shale and mudstone (see also Fig.3). Based on samples from the Bright Angel and Kaibab trails, plus literature descriptions (7,8), the breccia fragments can be traced largely to the Hermit Shale and Supai Group. Most pipe-fill sandstone occurs as breccia matrix, but large massive blocks of Coconino Sandstone have also been observed within the pipe (9). One fragment of oolitic, micritic limestone from the G stope, 365 level, could possibly have been derived from the Toroweap Formation. However, a similar-looking specimen was collected from the Supai Group, along the Kaibab Trail. Therefore, a Toroweap source for any of the breccia has not been determined with certainty.

Quartz sandstone and calcareous sandstone matrix

The breccia matrix consists of fine-grained subangular to subrounded quartz (>90%; average grain size 0.13 mm), with minor microcline and plagioclase. Near the pipe margins, the quartz content decreases and the matrix becomes more calcareous (up to 30-50% carbonate; average quartz grain size 0.14 mm; Fig.3). In parts of the pipe, much of the sandstone matrix is massive, with little or no breccia fragments (Fig.3).

Coconino quartz is readily distinguished from Supai or Hermit on the basis of average grain size distribution (Fig.4).

1) < 0.1 mm	Bleached and unbleached Supai, and Hermit Formations.
2) > 0.1 mm	Massive quartz and calcareous sandstone fill, breccia matrix, and Coconino Sandstone (from Grand Canyon trails).

The weighted average quartz grain size for the Supai samples examined in this report is 0.077 mm ±0.015 (N=17), that for pipe matrix is 0.14 mm ±0.013 (n=32), and that for the Coconino Sandstone (outside the pipe) is 0.13 ±0.03 (N=4). Comparison of the means, using the Student's T test, indicates that the average quartz grain sizes of the pipe matrix and Coconino samples are statistically identical, whereas the averages of matrix versus Supai (or Hermit) are significantly different at the 95% confidence level. These values do not support the Esplanade origin (1) for sandstone matrix, between the 75-450 levels.

245

Much of the Coconino sandstone appears to have been either weakly cemented or decemented at the time of collapse. Breccia fragments incorporated into bedded sandstone matrix probably resulted from filling of local cavities within the pipe by a slurry of loose sand and small rock fragments. Furthermore, Coconino quartz shows the greatest stratigraphic displacement among pipe fill materials, having been observed to the 430 level, or 630 ft (190m) below the Coconino-Hermit contact. This depth is a minimum estimate, as lower levels have not been sampled.

SiO_2 cementation of sandstone matrix may have occurred shortly after Coconino deposition, or later, after collapse of the loose quartz sand into the pipe. However, subsequent to collapse, carbonates filled the interstitial pore space within the matrix sand. Framework quartz grains are commonly unsupported and "float" in a coarse-grained (occasionally poikiolitic) calcite/ dolomite cement, which recrystallized from micritic calcite, relicts of which can still be seen in thin section. The open texture implies a high degree of porosity at the time of pipe-fill deposition.

The calcareous matrix cement may have been redeposited from carbonates dissolved from the upper Redwall Limestone, and lower Supai Group. Carbonate dissolution at depth would have provided space for the continuation of upward stoping. However, extensive dissolution of quartz and replacement by carbonates has not occurred at the mine levels under study, and thus massive quartz sandstone occurs intact in the pipe-fill (Fig. 3). Although, generally, calçite has only marginally corroded quartz along grain edges, some minor, localized occurrences of more thorough replacement have been noted.

Ore Mineralization and Paragenesis

Pre-ore alteration

That bleaching, or reduction of ferric oxides, probably preceded mineralization, is suggested by the enclosure of carbonate cement and ore minerals around the bleached materials. Hematitic haloes around uraninite (with associated sulfides) demonstrate a later iron-oxide overprint on already-bleached pipe-fill.

One may expect that the reduction of Fe^{+3} should produce an early generation of finely disseminated pyrite. This is supported by the presence of fine-grained cubic pyrite, evenly scattered in some breccia fragments, in contrast to coarser-grained subhedral to anhedral pyrite that replaced calcareous sandstone matrix. However, some of the observed textural differences of pyrite may have resulted from variations in porosity between clasts and matrix.

Recrystallization of carbonate cement in pipe fill also predated ore deposition, as the carbonates are a preferred site for massive ore replacement. The continued presence of dolomite in some heavily mineralized samples (e.g. 991-F-C85) suggests preferential replacement of calcite by ores. Crystallization of kaolinite into fibrous sheaves or rosettes may have been concurrent with or after carbonate recrystallization, since it commonly fills pore space between both quartz and calcite grains.

Early-stage mineralization

Barite was one of the first ore-related minerals to have formed after dolomite (Table I). Barite occurs as bladed or prismatic crystals, and as cement. Many of the larger barite crystals were replaced by pyrite and other sulfides. Barite was closely succeeded by siderite, which forms tiny clusters on both dolomite rhombs and barite blades. Although barite is predominantly an early phase, late-stage barite also occurs. For example, in sample 991-P-C86, barite has deposited <u>after</u> sulfides and uraninite.

Nickel/cobalt sulfides and arsenides also were deposited early in the sequence (Table I). Bravoite occurs as microscopic, brownish, isotropic cubes and octahedrons at the cores of pyrite cubes, and as thin bands in zoned pyrite (Fig.5). Much of the bravoite has decomposed or dissolved, leaving hollow casts. Siegenite also forms euhedral crystals in pyrite, or is enclosed by bravoite in pyrite. Gersdorffite appears in trace amounts in pyrite.

Nickel arsenides are less abundant, and occur in the annular ring. Nickeline (niccolite) is enclosed by rammelsbergite and pararammelsbergite. Rammelsbergite is euhedral, zoned, and has hollow cores that may have formed by dissolution of nickeline, in a manner analogous to the removal of bravoite within pyrite. These voids were partially filled later by bornite, digenite and covellite. An unidentified polymetallic sulfarsenide associated with rammelsbergite (Fig.6) was determined by microprobe analysis to contain Ni,

TABLE I. MINERAL PARAGENESIS OF THE ORPHAN MINE

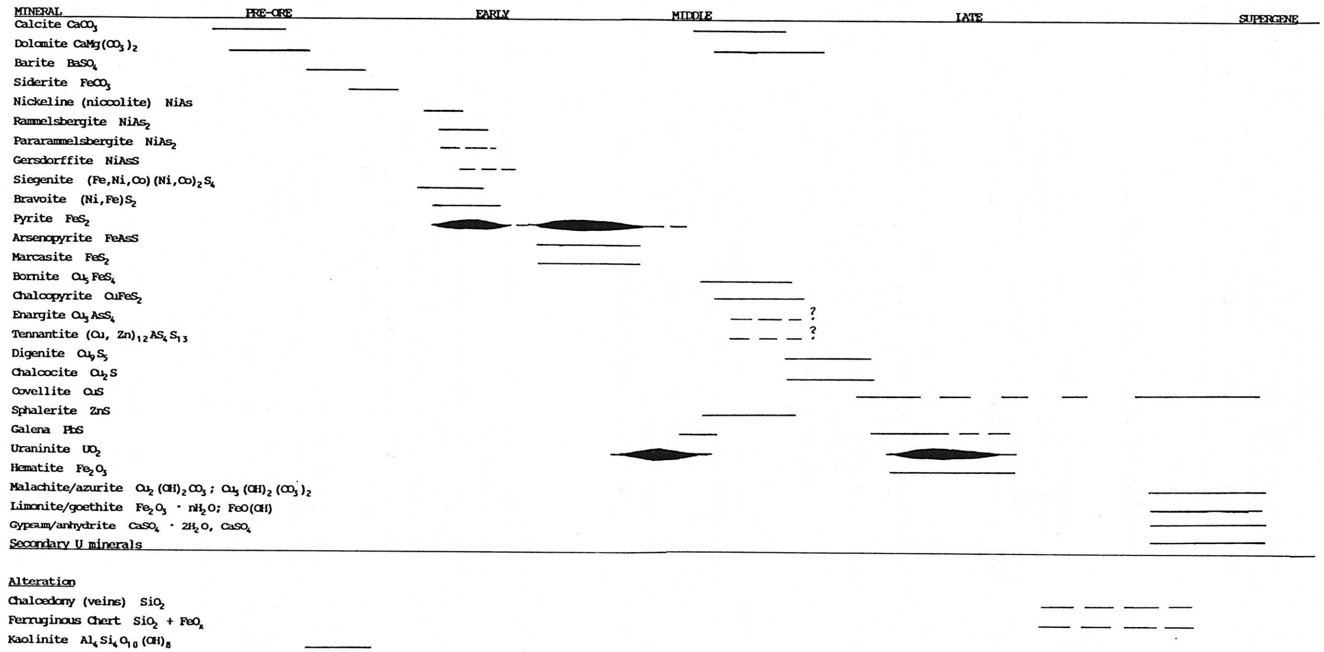

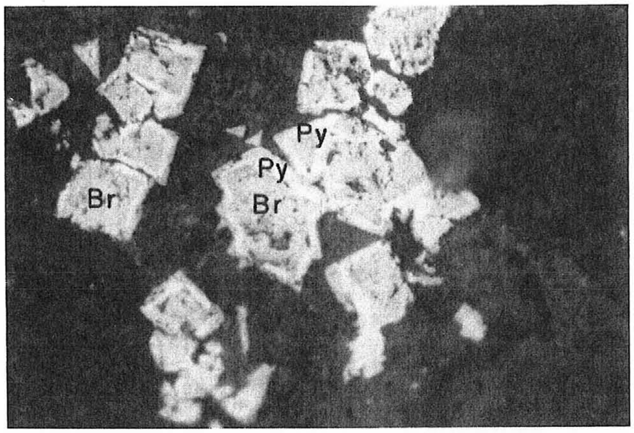

Figure 5. Zoned pyrite (Py) with bravoite cores (Br) (0.13 mm across).

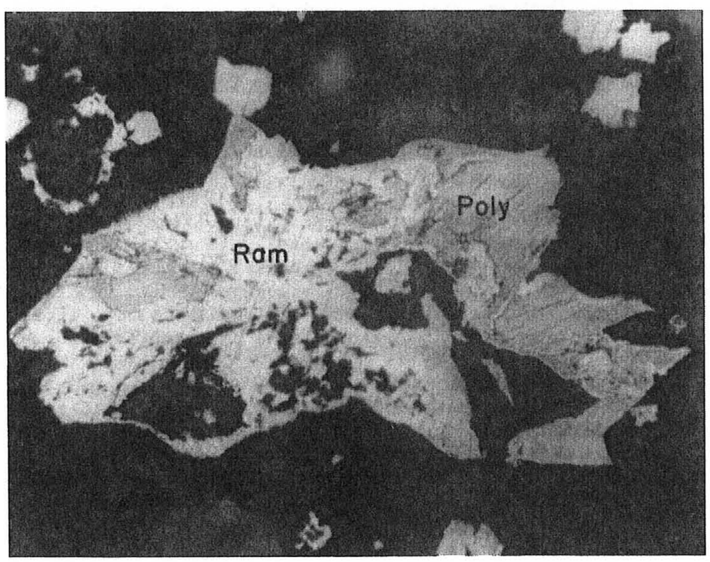

Figure 6. Rammelsbergite (Ram) with polymetallic phase (Poly), 420 level, annular ring (0.21 mm across).

Cu, with traces of Co and Zn. Other minute matrix crystals appear to be a mineral, as-yet unidentified, containing Cu, Zn, Ni, Co, S.

Pyrite is the most abundant sulfide mineral. Two discrete generations are present (Table 1). Early pyrite consists of very fine-grained, disseminated cubes, scattered interstitially between quartz grains, partly replacing cement, and cleavages of barite. This pyrite is strongly zoned, with cores and bands of bravoite and siegenite (Fig.5). Later, massive pyrite replaced carbonate cement within the pipe matrix, ultimately filling in cracks, and embaying quartz. A similar sequence is observed in sandstone deposits [Fig. 489 in (6)], and in other breccia pipes on the Colorado Plateau. Arsenopyrite and marcasite are usually found intergrown with massive pyrite.

Much of the massive pyrite is highly fractured. The fractures are filled with copper minerals such as digenite, chalcocite (Fig.7), and bornite as well as quartz and galena. Although fracturing could conceivably be linked to ore-related deformation and ore deposition, pyrite is the only sulfide which is strongly shattered. This may reflect the relative brittleness of pyrite, or crystallization pressure, due to emplacement of other ore minerals. For example, in several samples, intact detrital quartz grains are observed adjacent to fractured pyrite (e.g. sample no.1090/5630).

Middle-stage mineralization

Uraninite is the only primary uranium mineral. It forms thin coatings around quartz grains, less frequently, spherical or botryoidal masses (Fig.8), and in one sample from the 100 level, replaced silicified wood.

A very dark gray, isotropic phase occasionally appears as blebs or oriented blades along incipient shrinkage cracks in uraninite. Although microprobe analyses indicate that this dark phase is chemically identical with ordinary uraninite, it could be slightly more oxidized [p.1050 in (6)].

Botryoidal uraninite with shrinkage cracks filled by bornite and chalcopyrite clearly preceded these copper minerals (Fig.8). Due to inaccessibility of portions of the mine during field work as well as prior mining of high grade ore, it was not possible to determine the extent of early stage uraninite.

Copper minerals have succeeded massive pyrite (Fig.7,9) and early uraninite (Fig.8, Table I). Ragged pyrite inclusions remain in chalcopyrite, and bornite. Digenite and chalcocite are generally younger than either chalcopyrite or bornite. However, the relative paragenetic position of chalcopyrite vs. bornite, and digenite vs. chalcocite, varies from one section to another, suggesting that minerals within each pair formed more or less contemporaneously.

Chalcopyrite occurs as disseminated grains, oriented blades along (100) cleavage directions in bornite, and rims around bornite (Fig.8). The oriented blades are surrounded by a thin band of digenite. The relative proportions of chalcopyrite-bornite-digenite vary widely from grain to grain, less than several millimeters apart. In many grains the proportion of chalcopyrite to bornite is too great to be accounted for by exsolution. Therefore, these textures suggest replacement rather than exsolution.

Bornite commonly occurs in association with the other copper minerals. Tiny white blebs, identified as galena by microprobe analyses, occasionally appear in bornite (Fig.8). This galena may be older than the coarser grained galena found elsewhere.

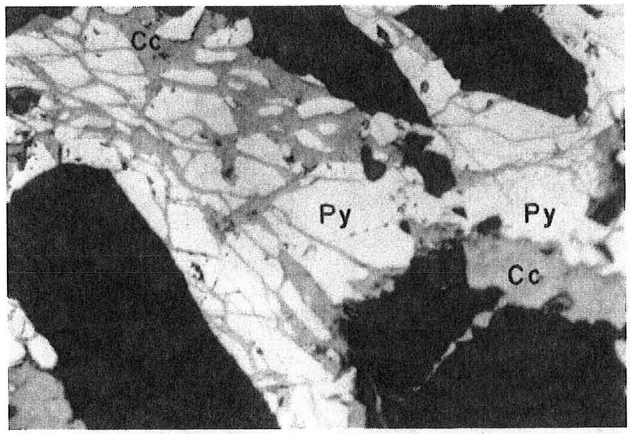

Figure 7. Highly fractured, massive pyrite (Py). Fractures are filled with chalcocite (Cc), 225 level (0.13 mm across).

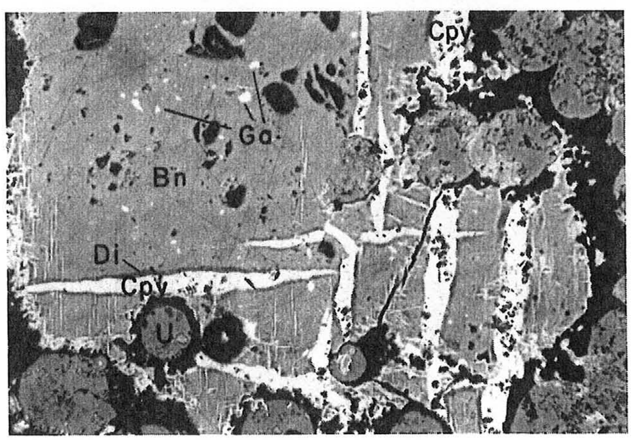

Figure 8. Botryoidal uraninite (U), with oriental blades of chalcopyrite (Cpy) and digenite (Di) in Bornite (Bn) in shrinkage cracks. Tiny blebs are galena (Ga), 420 level (0.45 mm across).

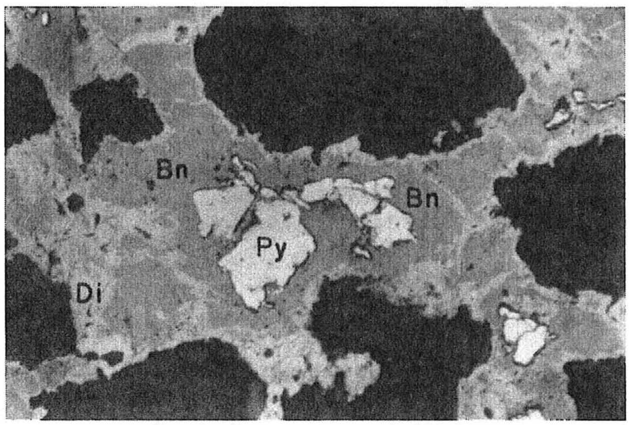

Figure 9. Pyrite (Py) remnants rimmed successively by bornite (Bn) and digenite (Di) (Thin section is 0.22 mm across).

Zn-bearing tennantite (identified by x-ray mapping on the electron microprobe) and enargite appear in trace amounts with the other copper minerals. Covellite replaces all other copper minerals, and is therefore the youngest copper sulfide.

Some carbonatization accompanied copper deposition. Digenite associated with dolomite is surrounded by later chalcocite (sample #11). Furthermore, large zoned calcite crystals, containing chalcopyrite inclusions, have been found (4).

Late-stage mineralization

That galena usually contains inclusions of pyrite, chalcopyrite, and sphalerite, but not the reverse, implies that galena crystallized after these minerals. The relative position of sphalerite is uncertain, but it is usually intergrown with galena and also contains inclusions of chalcopyrite.

A later stage of uraninite rims galena or copper sulfides indicating that it usually deposited after these minerals (Table I). However in some samples, galena appears to be younger than uraninite. The relatively late deposition of uraninite resembles the sequence observed at other mineralized Grand Canyon breccia pipes. Late-stage uraninite from the annular ring is often intergrown with base metal sulfides, nickel arsenides and hematite. These minerals tend to occur in discrete zones (Table II).

Table II. Summary of zonation in uraninite-hematite samples

	Hematite zone	bleached	transitional	uraninite zone
early				Ni sulfides and arsenides
	pyrite (rare)			pyrite
			bornite	bornite
	chalcopyrite	chalcopyrite (rare)	chalcopyrite	chalcopyrite
	digenite	digenite	digenite	chalcocite
	covellite		covellite	
	sphalerite (rare)			sphalerite
	galena (rare)			galena
	hematite			uraninite
late				(galena)

Supergene enrichment and secondary minerals

Secondary enrichment and oxidation may be related to the late Tertiary period of active dissection of the sediments (10). Some supergene enrichment of copper is suggested by the occurrence of chalcocite overlying chalcopyrite in the pipe (1), and replacement of other copper minerals by covellite. Partial oxidation of uraninite is also indicated by relatively small unit cell constants, suggesting a formula close to $UO_{2.34}$ (4). Fracture fillings of secondary minerals (e.g. malachite, gypsum, chalcedony), vugs of anhydrite or gypsum, and the diverse array of oxidized secondary minerals (3, 5) are probably associated with this episode.

Mineral Zonation

Uranium ore has accumulated in the annular ring, around the circumference of the pipe, as well as within the pipe. The distribution of ore within the pipe has been controlled by a combination of intrinsic lithological permeability and induced permeability through fracturing. Massive ore has preferentially accumulated in relatively porous sandstone pipe-fill, and calcareous sandstone matrix, and in more porous units within the Esplanade Sandstone adjacent to the pipe, relative to siltstone or shale breccia fragments. However, the last commonly contain fine-grained disseminated pyrite.

The location of stopes indicates that uraninite was deposited in economic grade quantities above the 365 level; the grade increased upward as the amount of associated galena increased. The highest grade uraninite was confined between the 225 level and the adit (0 level), in porous sandstone breccia matrix. The A stope at the stratigraphic level of the upper Esplanade Sandstone, above the 175 level, has yielded the highest grade ore (>1.5% U_3O_8), although rich ore also has been recovered from the center of the pipe (B and G stopes, Fig.3), and from the heavily brecciated northern pipe rim (No. 1 stope). Little commercial-grade ore was found below the 400 level, in the Wescogame Formation (Fig. 10).

Pyrite is disseminated throughout the vertical extent of the pipe. Uraninite, massive pyrite, and minor quantities of galena, sphalerite, arsenopyrite and marcasite have concentrated within the center of the pipe. Annular ring ore consists of a complex, very fine-grained assemblage of chalcopyrite, copper sulfides and nickel (cobalt) arsenides with uraninite and hematite (Fig. 10).

Copper mineralization accumulated to a greater extent below uranium between the 225 and 400 levels, than elsewhere in the pipe (Fig. 10). Chenoweth (1) found that copper minerals have concentrated in a lower-grade U ore zone, inside the higher-grade uranium ore zone of the annular ring. This pattern was best developed between the 225-350 levels. Chalcocite was more abundant than chalcopyrite on the upper levels of the annular ring (190-225 levels), whereas chalcopyrite became more prevalent between the 245-350 levels (1). However, the limited samples available in this study are insufficient to reconfirm the chalcocite-chalcopyrite zonation. The concentration of chalcocite above chalcopyrite would be consistent with some supergene enrichment. Not unexpectedly, oxidation has been more pronounced at the uppermost mine levels (1).

Nickel arsenides occur between the 400 and 420 levels, along the annular ring, on the north margin of the pipe. Barite and siderite are common within the northeastern half of the pipe (Fig. 10).

Geochemical Considerations

Bleaching

As mentioned above, hematite has been removed from red beds within and close to the Orphan breccia pipe, probably at an early stage, that preceded ore formation and long before the later stage of hematite associated with uraninite. A similar bleached (reduced) zone is observed in other breccia pipes, whether mineralized or not. This may suggest an independent, regional process although it is possible that bleached, unmineralized pipes have been mineralized in the past, but ore minerals have subsequently been removed by weathering or oxidation.

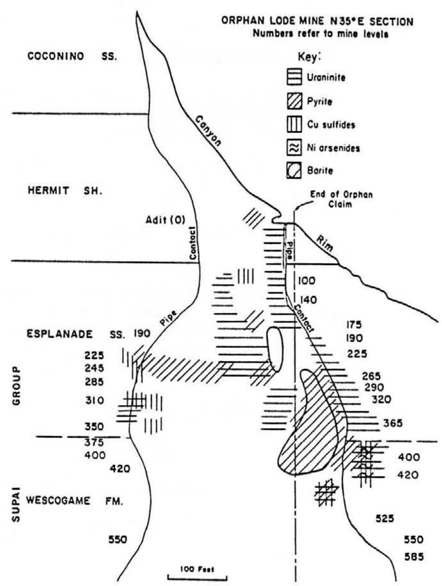

Figure 10. Cross-section of the Orphan breccia pipe, showing a schematic distribution of ore minerals.

The most likely reducing agents are organic compounds or H_2S. Only minor organic material is observed in the Orphan, mostly in plant fossils from the Hermit Shale and Esplanade Sandstone. Reduction of Fe^{+3} by H_2S is, therefore, more probable. A wide range of negative δS^{34} values suggests a sedimentary or bacterial origin for the sulfur (5). Bleaching by H_2S-bearing fluid and the precipitation of the early, finely-disseminated pyrite can be expressed by reactions such as:

$$Fe_2O_3 + 2 H_2S + 2H^+ = FeS_2 + Fe^{+2} + 2H_2O \quad (1)$$

Middle Stage Mineralization

Uranyl complexes carried by an oxidizing solution (11) may have been reduced by H_2S, pyrite, or other early sulfides and arsenides to form massive uraninite. For example:

$$4UO_2(CO_3)^0 + H_2S + 4H_2O = 4UO_2 + 4H_2CO_3 + H_2SO_4 \quad (2)$$

$$FeS_2 + 7UO_2(CO_3)^0 + 8H_2O = 7UO_2 + 7H_2CO_3 + Fe^{+2} + 2HSO_4^- \quad (3)$$

Cu sulfides appear next in the sequence. If Cu were carried as cuprous complexes (12), oxidation would have been required to form many of the observed ore minerals, perhaps by mixing of a base metal-bearing fluid with a more oxidizing solution. For example:

$$10Cu(HS)_3^{-2} + 2Fe^{+2} + \tfrac{1}{2}O_2 = 2Cu_5FeS_4 + H_2O + 6H_2S + 16HS^- \quad (4)$$

$$2Cu(HS)_3^{-2} + 2Fe^{+2} + \tfrac{1}{2}O_2 = 2CuFeS_2 + H_2O + 2H_2S \quad (5)$$

$$18Cu(HS)_3^{-2} + \tfrac{1}{2}O_2 = 2Cu_9S_5 + H_2O + 8H_2S + 36HS^- \quad (6)$$

$$2Cu(HS)_3^{-2} + \tfrac{1}{2}O_2 = 2CuS + H_2O + 4HS^- \quad (7)$$

Late Stage Mineralization

A second period of uranium deposition is characterized by the distinctive hematite-uraninite-base metal sulfide zonation discussed above (Table II). A plot of mineral stability fields as a function of log fO_2 vs. log fS_2, at 100°C, for a number of common-base metal oxides and sulfides (Fig.11), provides useful insights into the nature of the late stage hematite-uraninite zonation. The resultant stability fields shown in Fig.11 are compatible with observed mineral phases, and provide an overview of the probable ranges of oxygen and sulfur fugacities. However, because of data limitations, the time-variations in fO_2 and fS_2 levels have not been modelled here.

In Figure 11, the boundary between hematite and pyrite is defined by a diagonal line from the Py-Mt-Hm triple point, lower left, going to the upper right. The observed mineral zonation crosses this line. The concentration of chalcopyrite near the contact between hematite and bleached zones (Table II) is consistent with the location of its wedge-shaped stability field, on both sides of the hematite-pyrite boundary. The convergence of the fields for the other observed copper and nickel minerals into a fairly small area suggests deposition under a limited fS_2 gradient.

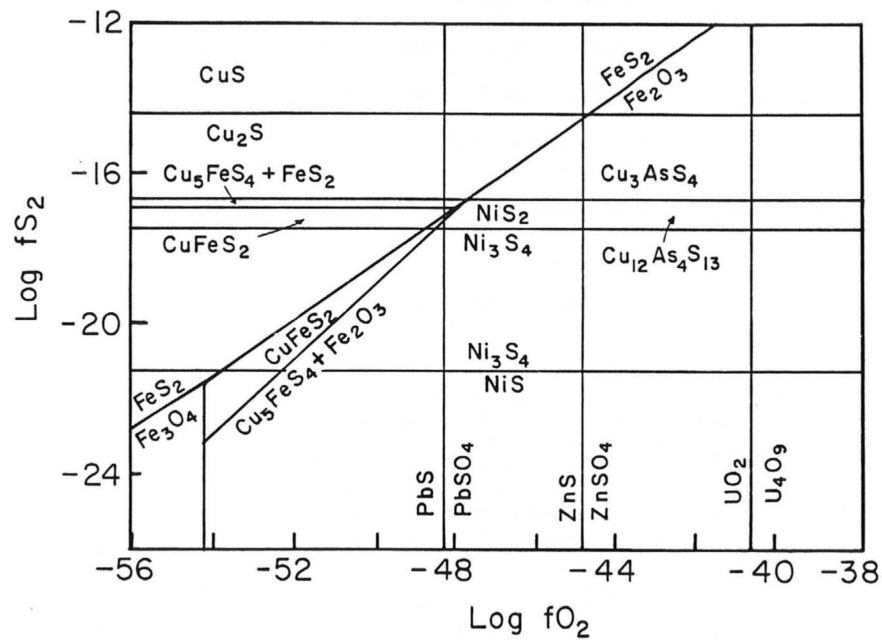

Figure 11. Mineral stability fields as a function of log fO_2 vs. log fS_2, at 100°C, for a number of common base-metal oxides and sulfides. The plotted minerals include hematite (Fe_2O_3), bornite (Cu_5FeS_4), chalcopyrite ($CuFeS_2$), pyrite (FeS_2), chalcocite (Cu_2S), covellite (CuS), galena (PbS), sphalerite (ZnS), uraninite (UO_2), U_4O_9, enargite (Cu_3AsS_4), vaesite (NiS_2), millerite (NiS), polydynite (Ni_3S_4), tennantite ($Cu_{12}As_4S_{13}$), anglesite ($PbSO_4$), and magnetite, Fe_3O_4.

The exact position of uraninite is determined by the stability of the uranyl complex, predominantly $UO_2(CO_3)^0$ at ~100°C (11). However, the univarient curve for the solid transition UO_2 - U_4O_9 is plotted instead, because of the availability of good thermodynamic data. The transition from UO_2 to uranyl complex plots well to the left of that line. Since uraninite and hematite do not co-exist in the zoned samples, and chalcopyrite has deposited <u>before</u> uraninite (Tables I, II), precipitation may have occurred under increasing fO_2 levels. The geometry of the mineral zonation therefore can be represented by a gradient in fO_2, higher at the hematite end, decreasing toward chalcopyrite, then uraninite, pyrite and nickel minerals. Some characteristic reactions may have been:

$$7UO_2(CO_3)^0 + FeS_2 + 8H_2O = 7UO_2 + Fe^{+2} + 2SO_4^{-2} + 7H_2CO_3 + 2H^+ \quad (8)$$

$$6UO_2(CO_3)^0 + NiAs_2 + 8H_2O = 6UO_2 + Ni^{+2} + 2AsO_4^{-3} + 6H_2CO_3 + 4H^+ \quad (9)$$

$$8UO_2(CO_3)^0 + CuFeS_2 + 8H_2O = 8UO_2 + Cu^{+2} + Fe^{++} + 8H_2CO_3 + 2SO_4^{-2} \quad (10)$$

$$4UO_2(CO_3)^0 + PbS + 4H_2O = 4UO_2 + Pb^{+2} + SO_4^{-2} + 4H_2CO_3 \quad (11)$$

Slightly further away, where the entering pore solutions retained a higher oxygen fugacity:

$$2Fe^{+2} + \tfrac{1}{2}O_2 + H_2O = Fe_2O_3 + 4H^+ \quad (12)$$

<u>Mineralizing Fluids</u>

The early bleaching suggests the passage of sulfide-bearing fluids early in the history of the pipes. The base metals (Cu, Ni, Pb, and Zn) may have also been transported by sulfide-rich fluids at a later time, although their total solubility in such solutions may be too low (11, 13). Alternately, they may have been carried by NaCl-rich brines, such as observed in fluid inclusions (14, 15). However, transport of uranium requires a different, more oxidized fluid, because uranium is sufficiently soluble only as uranyl (U^{+6}) complexes (11). The existence of sulfate for barite formation and the formation of later hematite also requires a more oxidizing fluid. Thus, at least two, and probably more different transporting fluids were necessary for the formation of mineral assemblages observed in the Orphan pipe.

The concept of combining different fluids within these pipes is quite plausible. The pipe structure would facilitate the mixing of solutions derived from different rock strata, in a way analogous to the intersection of permeable zones by a drill hole. The chemistry and flow rate of the solutions entering the pipe could vary significantly through geologic time.

<u>Comparison of the Orphan Pipe with Other Grand Canyon Breccia Pipes</u>

Breccia pipes and associated orebodies are remarkably similar throughout the Grand Canyon region, an area covering almost one-fourth of the state of Arizona. The diameters of all of the known breccia pipes fall within a narrow range of about 30 to 150 m. The grade and tonnage of the ore within the Orphan Mine is comparable to other pipes presently being mined, although the ore at the Orphan seems to have been more concentrated around the annular ring, whereas at other mines, the bulk of the ore occurs within the pipe.

Perhaps the most striking similarity lies in the paragenesis. The repeated recurrence of the same extensive suite of minerals at the Orphan and other pipes cannot be mere coincidence. The paragenetic sequence established here for the Orphan varies only slightly from that observed in other breccia pipe orebodies. In fact, the crystallization sequence is almost identical; the difference lies more with the percentage of each mineral phase deposited at a specific time in the paragenetic sequence of each pipe.

Some of the major similarities, and a few differences are summarized below: (1) U-Pb dating establishes a narrow period of U mineralization for the Grand Canyon pipes [between 220-200 ma (16)]. (2) The Orphan mine clearly contains an early phase of botryoidal uraninite. This was not originally observed in other pipes, but a careful check has shown that at least one of the other mines also was found to contain minor amounts of this early botryoidal uraninite. (3) The mottled hematite-uraninite banding associated with the late stage uraninite appears to be far more prevalent in the Orphan ore than in most other orebodies, although at least two of the other pipes have notable examples of such an association. (4) The final stage pyrobitumen that is densely concentrated in at least one pipe, and observed in several others, occurs only in trace amounts at the Orphan (1). (5) Early anhydrite associated with barite does not appear to be prevalent at the Orphan, as it is at several other pipes.

Temperatures of formation also show close affinities (17). Fluid inclusion studies of several pipes yield filling temperatures of 80-145°C in dolomite, quartz, and sphalerite, with high salinities averaging 15 wt % NaCl (14). At the Hack 1 and 2 mines, homogenization temperatures of fluid inclusions in sphalerite range from 93 to 115°C, and salinity between 9.9 and 16.4 wt % eq. NaCl (15). Temperatures of 70-80°C have been found for carbonates (18). Collectively, these temperatures are somewhat higher than the 60-110° from calcite (linked to copper stage mineralization) at the Orphan (5).

The stratigraphic level of the ore at the Orphan is somewhat lower than at most of the pipes on the north rim. Almost all of the ore from the Orphan came from the statigraphic level of the Esplanade Sandstone, although this could be in part attributed to the removal of the upper portions of the pipe by erosion. It is possible that ore had previously been concentrated in the upper Hermit or Coconino levels, but was subsequently removed by canyon downcutting. Nevertheless, many of the pipes on the north rim do not have ore extending down into the Esplanade Sandstone, and ore from one pipe that does only extends partially into the Esplanade. One other orebody on the south rim apparently has ore at the same lower horizon as the Orphan. These relationships suggest that, at the time of deposition, the Coconino and Hermit on the north rim were at lower topographic elevations in the basin, thereby permitting mineralization at a higher stratigraphic level.

This study was based on a relatively small number of samples. As more data become available from the opening of new mines, more similarities or disparities between pipes may become evident.

Conclusions

The Orphan breccia pipe formed by collapse of overlying sediments into a sinkhole or cavern within the upper Redwall Limestone, which initially developed 325 my ago (19). Petrographic study of pipe-fill and background samples collected along Grand Canyon trails establishes that the pipe-fill is derived from units within the Supai Group, Hermit Shale and Coconino Sandstone. Textural evidence suggests that the Coconino Sandstone was largely unconsolidated or decemented during collapse. The youngest pipe-fill material (in this case Coconino, since Toroweap or Kaibab units have not been positively identified) limits the upper age of the structure. Thus, the pipe could be as old as mid-Permian, well predating Triassic uranium mineralization (16). Alternatively, the Late Mississippian paleokarst may have been reactivated during the Triassic, under a monsoonal climate (20), which produced fluctuating water tables. Such hydrologic conditions would have promoted the formation of sinkholes (21), and would have facilitated further upward stoping.

The accumulation of uranium ore in the annular ring and within the pipe was strongly controlled by fracturing and permeability. High grade uranium ore concentrated above the 225 level, whereas copper mineralization accumulated below the 225 level. There is also some indication of lateral zonation of U and Cu along the annular ring zone (1). Annular ring ore consists of a complex assemblage of uraninite/hematite with base metal sulfides and arsenides. New phases detected in this study include Zn-tennantite and a multimetallic element phase associated with rammelsbergite.

The paragenetic sequence at the Orphan includes deposition of early Ni sulfides and arsenides, succeeded by two generations of pyrite: fine-grained cubes and massive pyrite. These early minerals were followed by botryoidal uraninite and later by chalcopyrite, bornite, spalerite, galena and copper sulfides. A later generation of uraninite may have precipitated by reactions with previously deposited sulfides, and reoxidation of ferrous iron at greater distances. The observed mineral paragenesis is consistent with mixing of at least two different solutions, enhanced by the permeable environment within the breccia pipe.

The paragenetic sequence of the Orphan is closely paralleled by other Grand Canyon breccia pipes. Homogenization temperatures of fluid inclusions also fall within the range observed at other pipes (5,15). Major differences are the near absence of bitumens or hydrocarbons and of early anhydrite at the Orphan.

Acknowledgments

The first author wishes to thank Drs. M. Prinz and M. Weissberg for permission to use the research ore microscope at the American Museum of Natural History, New York City. Discussions with Dr. G. Bowles (U.S. Geological Survey, Denver) and Dr. D. Pohl (American Museum of Natural History) have been very helpful. This study is part of a larger project on the breccia pipes of northern Arizona, funded by the Bureau of Indian Affairs, and the U.S. Geological Survey.

REFERENCES

1. W.L. Chenoweth, "The Orphan Lode Mine, Grand Canyon, Arizona, A Case History of a Mineralized, Collapse-Breccia Pipe" (U.S. Geol. Survey Open-file Report 86-510, 1986), 1-91.

2. M.E. Kofford, "The Orphan Ore Deposit" (Unpubl. Mine Report, 1956).

3. M.E. Kofford, "The Orphan Mine" in "Geology and Natural History of the Grand Canyon Region," Four Corners Geol. Soc. Fifth Field Conf., (1969), 180-194.

4. V.M. Gornitz, "Mineralization, Alteration and Mechanism of Emplacement, Orphan Ore Deposit, Grand Canyon, Arizona" (Ph.D. Dissertation, Columbia University, 1969).

5. V. Gornitz and P.F. Kerr, "Uranium Mineralization and Alteration, Orphan Mine, Grand Canyon, Arizona," Econ. Geol., 65 (1970), 751-768.

6. P. Ramdohr, The Ore Minerals and Their Intergrowths, vol. 2 (Oxford and New York: Pergamon Press, 1980), 1269 p.

7. E.D. McKee, "The Supai Group of Grand Canyon," U.S. Geol. Surv. Prof. Paper, 1173(1982), 1-504.

8. D. White, "Flora of the Hermit Shale, Grand Canyon, Arizona," Carnegie Inst. Washington, 405(1929), 1-221.

9. C.G. Bowles, private communication with author, U.S. Geological Survey, Denver, 24 February 1987.

10. C.G. Bowles, "Economic Implications of a New Hypothesis of Origin of Uranium and Copper-Bearing Breccia Pipes, Grand Canyon, Arizona," U.S. Geol. Surv. Circ., 753 (1977), 25-27.

11. D. Langmuir, "Uranium Solution-Mineral Equilibria at Low Temperatures with Applications to Sedimentary Ore Deposits," Mineral. Assoc. Canada Short Course in Uranium Deposits, ed. M.M. Kimberley (Toronto: U. Toronto Press, 1978), 17-55.

12. H.L. Barnes, "Solubilities of Ore Minerals," Geochemistry of Hydrothermal Ore Deposits, ed. H.L. Barnes (New York: Wiley-Interscience, 1979), 404-460.

13. H.L. Barnes, "Ore-Depositing Reactions in Mississippi Valley-Type Deposits," Proc. International Conf. on MVT Pb-Zn Deposits, eds. Kisvarsanyi et al. (Rolla, Mo: University of Missouri, 1983), 77-85.

14. K.J. Wenrich, and L.M. Pratt, "Paragenesis and Conditions of Formation of Ore Minerals from Metalliferous Breccia Pipes, N. Arizona," G.S.A. Abstr. and Prog., 17 (1985), 747.

15. J.D. Rasmussen, C.G. Cunningham, and A.M. Gautier, "Primary Fluid Inclusions in Sphalerite from the Hack 1 and 2 Mines, Mohave Co., Arizona," G.S.A. Abstr. and Prog., 18(5)(1986), 404.

16. K.R. Ludwig, J.D. Rasmussen, and K.R. Simmons, "Age of Uranium Ores in Collapse-Breccia Pipes in the Grand Canyon Area, Northern Arizona," G.S.A. Abstr. and Prog., 18 (1986), 392.

17. K.J. Wenrich, "Mineralization of Breccia Pipes in Northern Arizona," Econ. Geol., 80 (1985), 1722-1735.

18. P. Landais, "Geochemical Analysis of the Organic Matters Associated with the Breccia Pipes in the Grand Canyon Area," G.S.A. Abstr. and Prog., 18(5)(1986), 389.

19. G. Billingsley, "Relations of the Surprise Canyon and Watahomigi Formations to Breccia Pipes in the Grand Canyon, Arizona," G.S.A. Abstr. and Prog., 18(5)(1986), 342.

20. R. Dubiel, "Sedimentology of the Upper Triassic Chinle Formation, Southeastern Utah" (Ph.D. Dissertation, University of Colorado, 1987), 1-125.

21. B.F. Beck, R. Ceryak, D.T. Jenkins, T.M. Scott, and D.P. Spangler, "Karst Hydrogeology of Central and Northern Florida, Field Guidebook," (Report 85-86-1, G.S.A. Annual Meeting, Orlando, Florida, 1985).

With the compliments of the authors.

Reprinted from:

PROCESS MINERALOGY VII-AS APPLIED TO
SEPARATION TECHNOLOGY, 1988

edited by:

A.H. Vassiliou, D.M. Hausen, and D.J. Carson

The Metallurgical Society
Warrendale, PA

SCANNED
NJN 2008

Exploration Geology of Canyon BrecciaPipe
South of Grand Canyon, Arizona

William P. Casadevall, Energy Fuels Nuclear
(Lecture presented at Oct. 1989 AAPG meeting in Albuquerque, New Mexico)

The Canyon Pipe was discovered in 1978, and its occurrence is typical of numerous solution-collapse breccia pipes in northern Arizona. Collapse appears to have occurred in several distinct episodes stoping up to and sometimes through the Triassic Moenkopi, a vertical distance of over 2300 ft vertical feet. There was little exploration interest in the area until the late 1970's when a few companies realized that the compact high-grade orebodies provided an attractive target in a declining uranium market. The structure, alteration, and the nature and distribution of mineralization at the Canyon are quite similar to that described for the Orphan.

The Canyon breccia pipe is located in Kaibab National Forest 13 miles south of the Grand Canyon and the Orphan mine. The surface expression of the Canyon pipe is a broad, shallow, structural basin in the Permian Kaibab Formation over 1/2 mile in diameter. The basin formed by depletion of soluble material in the Kaibab and Toroweap Formations by ground water moving in toward the pipes. Correlations with drill holes on the margin of the basin show over 20% of the section has been removed primarily in the Toroweap horizon. The center of the basin is filled in with Triassic Moenkopi redbeds. The pipe is essentially vertical and can be divided into two zones: (1) the collapse cone refers to that area of the Kaibab and Toroweap horizons, which have been affected by the formation of the pipe, more specifically the zone of depletion and the thinning of these units approaching the pipe. Drill hole data usually correlates fairly well through this zone and matrix dominant breccia appear most common; (2) the pipe throat is that portion which has undergone catastrophic collapse--in this portion of the pipe the pipe wall rock contacts are generally sharp; clast dominant breccias seem to predominate. Drill hole data do not correlate well, but do reflect vertical changes in the lithology--for example the change from Toroweap to Coconino to Hermit dominant breccias. From an exploration standpoint the definition of the collapse cone is the initial objective with the pipe throat usually being associated with the center of the collapse. In the upper portions, the throat of the Canyon Pipe is defined by downdropping of the Moenkopi-Kaibab and Toroweap-Coconino contacts and the lack of correction in between. Out away from that zone you get into units correlating better in your drill holes, but its generally the collapse cone that is very poorly defined. The boundary of the pipe in the Coconino horizon is poorly defined with core samples suggesting the zone is dominated by very large blocks of Coconino that are over 150 feet tall, which have been downdropped with minimal rotation.

Drill hole data allow good definition of the pipe through the ore horizon, the main zone of interest, which is middle Coconino through middle Esplanade. This coincides with the portion of the Orphan pipe left intact after erosion. The pipe diameter at the Coconino-Hermit is approximately 80 feet being slightly larger at the Hermit-Esplanade. As at the Orphan the pipe flares dramatically in the Esplanade horizon becoming kidney-bean shaped 120-150 across. The Canyon pipe is approximately 1/2 the diameter of the Orphan.

Reducing conditions predominate below the Moenkopi, chacaterized by an average of 5% Fe sulfides. Thin zones of more massive pyrite are found along fractures and scattered throughout the pipe being especially concentrated in a zone near the Toroweap-Coconino contact. This sulfide cap is composed primarily of pyrite with lesser amounts of bravoite, a Ni-Fe-sulfide. The cap averages 20 ft thick becoming thicker and deeper toward the center of the pipe. The dramatic thickening of the sulfide cap over a short horizontal distance which was noted in two drill holes, suggests an internal collapse. In the Kaibab and Toroweap horizons reducing conditions grade outwards for over a large distance into essentially unaltered sediments. Below the sulfide cap is a prominant zone of oxidation in which Fe sulfides are altered to Fe oxides. This zone is thinnest in the center of the pipe less than 5 feet beneath the thickest sulfide cap spanning outwards from that point--it grades outward into essentially unaltered Coconino. In the Hermit and Lower Supai horizons the pipe material is reduced. The normally redbeds adjacent to the pipe are bleached. There are some indications of secondary alterations. Redox boundaries are remobilized in towards the pipe by groundwaters. Copper carbonates are common in this zone and the potential exists here for redistributed ore. In the lower portions of the pipe reducing conditions exist, although the alteration of clasts is sometimes incomplete. Silicification is especially strong in through the center of the structure. Uranium mineralization extends from the Lower Toroweap to the Upper Redwall horizons--a vertical distance of over 1700 feet. As at the Orphan, ore grade mineralization occurs from the middle of the Coconino to the Lower Esplanade horizons but is also found scattered through the Lower Supai. Strongest mineralization in both pipes occurs in the Lower Hermit-Upper Esplanade horizons in a fairly narrow band at the pipe margin. At the Orphan this annular ore zone varies in width from 6 to 50 feet; inclined continuous core holes at the Canyon indicate a similar width. Mineralization inside the pipe occurs in the matrix portion of the breccia; outside the pipe mineralization occurs in fractures in relatively undisturbed sediments. Mineralization inside the Canyon pipe is generally not concentrated in the most permeable zones. Breccias derived from the Coconino sands and finely comminuted Hermit Shale appear most favorable. Some examples of mineralized intercepts from surface drill holes includes 88 feet of 0.42%, 41 feet of 0.81% and one hole containing 44 feet of 2.22%. In many other pipes particularly those north of the Grand Canyon mineralization occurs within the pipes often controlled by internal collapse structures. Although better known for its annular orebodies the Orphan also has a sizeable internal orebody. Drilling at Canyon did not indicate an economic orebody inside the pipe. No brecciated mineralization, which might indicate an internal collapse, has been noted. In the weaker ore zones the uraninite and pitchblende occur in very fine disseminations and coatings on individual sand grains. In the high grade zones uraninite typically occurs around the pyrite core whcih in turn envelopes earthy red hematite. Recent petrographic work shows that the hematite is an oxidation product--not primary as originally believed. Zones of massive copper sulfides often are found in and below the massive Hermit ore zones. These copper sulfides often replace high grade uranium mineralization. Galena and sphalerite also occur and geochemical data indicate Mo, Co, Ni, and As, observed in other pipes are present, although no zoning has been worked out. Several stages of barite have been noted with pale yellow radial barite being most typical.

Calculated reserves at Canyon are 66,600 tons of ore containing nearly 1,000,000 pounds of uranium with an average grade of 0.72%. 90% of those reserves are in the Esplanade ore horizon.

To summarize: The exploration data shows that the Canyon pipe formed during several periods of collapse. At the surface the pipe forming process affected an area over 1/2 mile in diameter. The structure is essentially vertical and nearly circular in plan view. The throat of the pipe is considerably larger in the lower horizons. Ore grade mineralization is concentrated along the margin of the pipe both inside and outside of the structure. Ken Ludwig has calculated a Pb-U age date of 260 Ma for the mineralization at Canyon--this is the oldest dated breccia pipe deposits in the region and indicates that mineralization at Canyon was emplaced as pipe formation continued.

WESTERN GOLD & URANIUM, INC.
42 BROADWAY
NEW YORK 4, N. Y.

WHITEHALL 4-6478

SILVER REEF URANIUM MINES
OFFICE: LEEDS, UTAH

FIRST NATIONAL BANK BUILDING
CARSON CITY, NEVADA

December 14, 1955

TO THE STOCKHOLDERS:

Two notable developments in the company's recent operations make this interim report to shareholders advisable.

First, the ORPHAN property of Golden Crown Mining Co., in which Western owns a controlling interest, has now proved to be a primary uranium strike of major proportions. Diamond drilling thus far has not been sufficient to prove the entire structure. However, the company's geological staff has indicated that the structure is of a pipe nature; mineralization has occurred around the perimeter of the structure with mineable vein widths of 30 to 40 feet. The deposit is in a mineralized shear zone of Coconino sandstone of Permian age. The mineral is pitchblende.

Thus far an ore body of not less than 100,000 tons is indicated, but your management believes that ore may well reach 300,000 tons or more (based on a minimum of 500 feet of perimeter X vein width of 30 feet X vertical height of 280 feet = 4,200,000 cubic feet, divided by 14 cubic feet per ton = 300,000 tons.) At an average probable grade of .45% uranium oxide, anticipated profits would be approximately $30 per ton.

The foregoing expectations do not include possibilities for additional depth and height (hole No. 11 went down 217 feet and was still in the mineralized area), nor the possibility of finding ore within the heart of the pipe structure.

The Orphan thus appears to be one of about 25 uranium finds in the U.S. of more than 100,000 tons, and also one of the very few sizeable pitchblende deposits found in this country. Because the ore body is many times the size originally expected, initial production will be delayed somewhat, with the first ore to be marketed in the spring. It will be trucked 85 miles to the new AEC ore-buying station at Tuba City, Arizona.

Secondly, since our September 26 report, Western has started to develop its SILVER REEF property in Southwestern Utah, where 36,000 tons of uranium-silver ore has been blocked out. A 125-foot shaft to the ore body is well under way and will be completed in about two months. A new hoist house has been constructed near the shaft and the hoist installed; a carpenter shop, change room, water tank and oil tank also have been installed. Initially, that portion of the ore high in uranium content but low in silver will be shipped to an AEC ore-buying station, while the silver-rich ore will be shipped to a silver smelter. The great bulk of the ore, which contains about equal values of uranium and silver, will, however, be held for treatment in a silver flotation mill to extract the silver before it is shipped to the AEC. A 50-ton-a-day mill will be built next spring.

For your further information, we are enclosing a detailed summary of the company's present status which we believe will be both interesting and helpful.

Respectfully submitted,

Ralph G. Brown

Ralph G. Brown
President

1986 GSA ABSTRACT FORM

USE THIS FORM FOR ALL 1986 GSA MEETINGS (SECTION & ANNUAL MEETINGS)

YOU MUST COMPLETE ALL SECTIONS BELOW, 1 THROUGH 7

1 TYPE YOUR ABSTRACT IN THE SPACE BELOW, using fresh black carbon ribbon. Follow the format shown on the attached instructions. Blue lines below show **absolute** limits. *Do not fold abstract*; mail flat with reinforcement to avoid retyping charge.

No 86525

THE ORPHAN LODE: A CASE HISTORY OF A URANIUM MINE IN A BRECCIA PIPE, GRAND CANYON, ARIZONA

CHENOWETH, William L., Consulting Geologist, 707 Brassie Drive, Grand Junction, CO 81506

The Orphan Lode is a single, patented mining claim within Grand Canyon National Park. The claim was located for copper in 1893, below Maricopa Point on the south rim. Uranium was noted in the old workings by the USGS in 1951. The claim was leased in 1953 and a detailed geological examination determined the mineralization was in a collapsed structure. On the basis of a few drill holes and favorable geology, an aerial tram was built and production commenced April 1956.

Continued exploration and mining indicated that the ore-bearing structure was a circular, nearly vertical, breccia pipe with a mean diameter of 350 ft, which penetrated the Permian and Pennsylvanian rocks of the Grand Canyon. Ore bodies occurred around the pipe border (annular ring) and in the breccia within the pipe. Uraninite was the principal ore mineral. Chalcocite, tennantite, chalcopyrite, pyrite and galena were locally common, especially in the annular ring.

Public Law 87-457, enacted in May 1962, permitted underground mining off of the claim in the National Park, in exchange for title to the claim in 25 years. When mining ceased in 1969, mine workings had explored the upper 585 ft of the pipe. Drilling confirmed the pipe bottomed in a cavity within the Redwall Limestone. During the period 1956-1969, the Orphan Lode produced 4.26 million pounds uranium oxide, 3,400 pounds vanadium oxide, 6.68 million pounds of copper, and 107,000 ounces of silver.

2 ALL ABSTRACTS — INCLUDING SYMPOSIA ABSTRACTS — MUST be categorized into ONLY ONE of the 34 disciplines below. Do *not* add to the list. Choose the ONE discipline in which peer reviewers would be *best* qualified to evaluate your abstract. This does not necessarily determine the final technical session assigned.

- ☐ 1 archaeological geology
- ☐ 2 coal geology
- ☐ 3 economic geology
- ☐ 4 engineering geology
- ☐ 5 environmental geology
- ☐ 6 general geology
- ☐ 7 geochemistry
- ☐ 8 geology education
- ☐ 9 geomorphology
- ☐ 10 geophysics
- ☐ 11 geoscience information
- ☐ 12 glacial geology
- ☐ 13 history of geology
- ☐ 14 hydrogeology
- ☐ 15 marine geology
- ☐ 16 mathematical geology
- ☐ 17 micropaleontology
- ☐ 18 mineralogy/crystallography
- ☐ 19 oceanography
- ☐ 20 paleontology/paleobotany
- ☐ 21 petroleum geology
- ☐ 22 petrology, experimental
- ☐ 23 petrology, igneous
- ☐ 24 petrology, metamorphic
- ☐ 25 petrology, sedimentary
- ☐ 26 planetary geology
- ☐ 27 Precambrian geology
- ☐ 28 Quaternary geology
- ☐ 29 remote sensing
- ☐ 30 sedimentology
- ☐ 31 stratigraphy
- ☐ 32 structural geology
- ☐ 33 tectonics
- ☐ 34 volcanology

DETACH FOR MAILING

3 SESSION TYPE:

☐ This abstract was invited for the symposium titled ______

If you checked "symposium" above, skip the rest of this item and go on to item (4).

☐ Poster Session ☐ Oral session ☐ Either type

If you checked "Oral" or "Poster" above, the Program Committee may have to change the type of presentation due to time/space limits; therefore, check one of the following:

☐ I will accept a change of session type if necessary.

☐ Withdraw my abstract rather than change session type.

4 % OF THIS PAPER PREVIOUSLY PRESENTED ______

WHERE AND WHEN ______

5 CAN YOU BE A SESSION CHAIRMAN? ☐ Yes

Topic ______

Your name ______

Telephone (late June/early July) ______

6 SPEAKER'S IDENTITY AND MAILING ADDRESS:

Speaker's status (check one):

1 ☐ GSA Mem or Fel
2 ☐ GSA Student Assoc
3 ☐ Professional geologist (but not GSA mbr)
4 ☐ Student (not GSA Assoc)

Speaker's name

Address

Address

City State Zip

Country

Office Telephone: ( ) ______

Home Telephone: ( ) ______

Dates we can reach you: ______

7 SEND ORIGINAL + FIVE COPIES OF ABSTRACT TO APPROPRIATE ADDRESS SHOWN ON INSTRUCTIONS SHEET AND ON BACK OF THIS FORM. ALL ABSTRACTS MUST ARRIVE ON OR BEFORE DEADLINE SHOWN FOR EACH MEETING.

THE GEOLOGICAL SOCIETY OF AMERICA 1888

ORPHAN LODE URANIUM DEPOSIT

Size-grade summary

Compiled and interpreted by

W. I. Finch from Chenoweth (1986)

1987

① 1/22/87 WJ

Orphan Lode deposit Uranium size-grade data (Chenoweth, 1986)

Total for pipe:

		Tons rock	Ave grade	lbs U_3O_8
% recovery?	Mined ore 0 - 365 level	495,107 (+)	.43	4,257,571
	Unmined ore above 400 Level	227,273 calc	.11	500,000
	Low-grade material 500 - 1100 levels	9,500,000	.021	3,999,000
	Total	10,222,380	0.043 calc	8,756,571

Ore bodies:	tons ore	lbs U_3O_8	Average grade
Within pipe fill: Stope A			
Within pipe fill: Stope B			
Within pipe fill: Stope G Downward extension of B			
Annular ring, in part No. 1 stope			
Unmined above 400 in center of pipe			
Low-grade 500-1100 level ½ doz ore bodies, thin intercepts in cores, Big halo			
See Figs 20, 21, over ½ of ring — Wescogame ore 420-430 level, lower grade			

② Oriphan Lode   Cu, V, Ag, and $CaCO_3$ grade and size data   1/27/87 wy

(Chenoweth, 1986)

Grade based on 350 lb sample old Hogan adit:

0.217 % U_3O_8
1.47 % V_2O_5
0.81 % Cu
3.6 oz/ton Ag

Production 1956 - 1958 (Table 4)

% V_2O_5 = ~0.015   % $CaCO_3$ = range 0.30 - 14; weighted Ave =

Production 1958 4th Qtr 936 tons ore, 1.72 % U_3O_8, % Cu = 0.17

Table 2 p 38 - 1964 production 592,017 lbs U_3O_8

63,994 tons ore @ ave Cu = 1.30% =   lb

sulfide concentrate = 20 % Cu, 10 oz Ag/ton.

p. 43 Vanadium

1956 - Mar 1958   3,283 lbs V_2O_5

Copper

6,680,000 lbs Cu produced

Silver

107,000 oz produced

calc.

1962 - 1969   ore = 222,910   Cu & Ag recovered

1.10 - 1.50 % Cu, ________ lbs Cu

0.35 - 0.45 oz/ton Ag, ________ oz Ag

③ Orphan Lode deposit - ore body geometry (Chenoweth, 1986) 12/7/81 WJ

A ore body (within pipe fill)

Dimensions:

Height: 190 ft

Width: 40 ft max at 175' level

Length:

Location: NE part of pipe Host: Coconino sand fill

Grade: > 1.50 % U_3O_8

B ore body (within pipe fill)

Location: center of pipe Host: Coconino sand fill & Claystone breccia,

Dimensions:

Height 275' (+30 level to 245 level)

Width } diameter ~ 200' from 140 - 245' levels

Length

Grade:

Some high grade (> 1.00 % U_3O_8) pods

G ore body (within pipe fill)

Location: center with rake to NE below 245' Host: Breccia from Hermit, Esplanade, as well as some Esplanade sand fill.

Dimensions: (essentially a downward extension of B ore body

Height 120 ft (245 - 365 level)

Width } Max mean diameter of 160 ft on 320 ft level

Length

Grade: not as high grade as B.

Ore stringers from B & G coalesce with annular ring ore bodies in northern portion of pipe.
Small pods at 245, 265, 290, 320, & 365 levels.

Annular ring ore

Location:

Dimensions:

plus ore pods on 420-430, 525, 585

Height 395 ft, 190 - 420 ft levels / ranges from continuous to discontinuous

Width: 6 - 60 ft, generally 15 ft

Length: 800 of circumference. (fig 27 measurement)

310 - 350 level ore very wide, continuous between levels on NE but separated by 7-10 ft of barren mudstone on SE & S; bottom marked by mudstone.

Host: Esplanade - relatively undisturbed.

1) Peripheral shear ore below 400 level in SS of Wescogame

2) pipe fill adjacent to shear

3) undisturbed but arcuate faulting outside pipe fill.

No. 1 Stope 225 - 365 ft levels

Envelope of calcite cement extends completely around pipe from 190 - 585 level, and possibly below; it is largely outside the peripheral shear zone and has a maximum width of 60 feet

Registered
Professional Geologist
Wyoming Reg. No. PG – 269

WILLIAM L. CHENOWETH

Consulting Geologist

707 Brassie Drive
Grand Junction, CO 81506-3911
(970) 242-9062 (voice & fax)

May 17, 1999

Nyal Niemuth
Arizona Dept. of Mines and Mineral Resources
1502 W. Washington
Phoenix, AZ 85007

Dear Nyal:

In a separate map tube, I am shipping you some more maps from the Orphan Lode uranium mine in the Grand Canyon, Coconino County. These maps are listed on the enclosed sheet.

Sincerely,

Bill

ORPHAN LODE
Coconino County Arizona

Copies of Company Level Maps Showing
Production Grades Scale 1" = 20'

Most Levels Are Color Coded By Grade

LEVELS

225
245 (2)
260 - 265
285
285 West
290
310 - 320
320
335
350 - 365
420
430 (2)
525
550
585

Registered
Professional Geologist
Wyoming Reg. No. PG – 269

WILLIAM L. CHENOWETH

Consulting Geologist

707 Brassie Drive
Grand Junction, CO 81506-3911
(970) 242-9062 (voice & fax)

April 21, 1999

Nyal:

Enclosed please find my files on the Orphan Lode uranium mine in the Grand Canyon, Coconino County, Arizona.

I am very pleased that the Department will take these files along with the maps I previously sent you

Sincerely,

Bill

Field No.	Lab. No
4335X	4648
4336X A&B	4649A&B
4337A	4650
4337B	4651
4337C	4652
4337D	4653
4337E	4654
6337F	~~4~~4655

Lab. (Thin Sect.)
Nos. of Orphan samples.

Sample Number	Mine Level	Pol. Sect.	Pol. Slab	Pol. Plug	Geo-chem.		
991-265-2	265	X		X	X	5989	5536
991-320	320	X				5938	5518
991-320-1	320	X			X	5996	5709
991-320-2	320	X			X	5996	5709
991-320-4	320	X			X	5979	5701
991-320-6	320	X			X	5970	5697
991-320-7	320	X			X	6003	5695
991-320-8	320			X	X	5965	5686
991-320-8R	320				X	5965	5686
991-350-1	350	X			X	5743	5756
991-350-2	350	X			X	?	?
991-350-21	350			X	X	5770	5725
991-350-365	350-365	X			X	6034	5470
991-365-1	365				X	6144	5524
991-365-15	365	X				?	?
991-365-2	365	X				6130	5550
991-365-3	365	X			X	6130	5550
check 991-365-Sta9-10	365	X			X	?	?
991-365-X	365	X			X	6069	5505
991-365-XR	365				X	6069	5505
991-365-Y	365	X			X	6069	5505
991-375-D-1	375	X			X	5834	5367
991-400-1	400			X(2)	X	6056	5567
991-400-1R	400				X	6056	5567
991-400-30	400	X		X	X	?	?
991-400-R1	400				X	5622	6093
991-400-R2	400	X				5624	6095
991-400-R3	400	X			X	5626	6097
991-400-R4	400			X	X	5625	6096
991-400-~~X~~ 2	400	X				?	?
991-430-4A	430	X				6108	5617
991-430-4B	430			X		6108	5617
991-430-5	430			X(2)		6108	5617
991-525-33	525	X			X	6045	5650
991-550-2	550			X(2)		6138	5627
~~991-400-30~~		~~X~~		~~X~~	~~X~~	~~?~~	~~?~~

MISSING ~~ON THIS LIST~~

FOUND

#12 400 Level
Chalcopyrite, massive

#9 400 Level
Chalcopyrite from
uraninite - hematite ore

Sample Number	Mine Level	Pol. Sect.	Pol. Slab	Pol. Plug	Geo-chem.		
991-585-3	585			X		6130	5700
991-585-31	585			X		6127	5701
991-585-32	585	X			X	6125	5702
991-585-33	585	X			X	6124	5703
991-585-33A	585	X			X	6124	5703
991-585-33B	585	X			X	6124	5703
991-585-34	585	X		X	X	?	?
991-A-C84	(dump)	X				NA	NA
991-B'-C85	240	X					
991-B-C85	240	X			X		
991-C'-C85	310	X					
991-C-C85	310	X					
991-D'-C85	310	X					
991-D-C85	310	X			X		
991-DUMP1-C87	dump	X					
991-DUMP2-C87	(dump)	X					
991-E'-C85	310	X					
991-E-C85	310	X			X		
991-F'-C85	310	X					
991-F-C85	310	X			X		
991-G'	350	X					
991-G-C85	350	X			X		
991-H'-C85	450	X					
991-H-C85	450	X			X		
991-I'-C85	450	X					
991-I-C85	450	X			X		
991-J'-C85	outer annular ring	X					
991-J-C85	outer annular ring	X			X		
991-K-C85	?	X			X		
991-M-C86	100	X					
991-O'-C85	400	X					
991-O-C86	400	X					
991-P-C86	?	X					
991-Q-C86	175	X				5939	5581

Sample Number	Mine Level	Pol. Sect.	Pol. Slab	Pol. Plug	Geo-chem.		
991-R-C87	80	X			X	NA	NA
991-S-C87	80	X			X		
991-T-C87	0-15				X		
991-U-C87	0	X			X		
991-W-C87	0	X			X		

? = Can not locate sample location

NA = No location available

updated 9/20/94

Sample Number	Mine Level	Pol. Sect.	Pol. Slab	Pol. Plug	Geo-chem.	COORDINATES NORTH	EAST
1000/5557	175	X				6000	5557
1090/6630	400	X				6090	5630
✓ 11			X			?	?
1150/5480	420	X(2)				6150	5480
1190/5630	585	X				6190	5630
✓ 12	400		X			?	?
✓ 4			X			?	?
✓ 5			X			?	?
5′	190	X				5511	5972
6′	400	X				6100	5629
7	225	X				5322	5910
760/5680	350	X				5760	5680
8	420		X			5960	5665
8′	400	X				6113	5632
✓ 9	400		X			?	?
900/5658	290	X				5900	5658
✓ 991-0-2	0			X	X	?	?
✓ 991-0-3A	0	X			X	?	?
✓ 991-0-3B	0	X			X	?	?
✓ 991-00-1	0	X			X	?	?
991-175-1	175	X			X	6014	5524
991-190-1	190				X	5942	5588
991-225-4	225	X			X	6015	5562
991-245-0-2	245			X		5842	5430
991-245-1	245	X				5920	5531
991-245-10	245	X			X	5842	5420
✓ 991-245-11	245	X			X	?	?
✓ 991-245-11C	245	X			X	?	?
991-245-2	245				X	?	?
991-245-4	245			X		5792	5386
991-245-4A	245				X	5792	5386
991-245-4B	245				X	5792	5386
991-245-5	245			X	X	5794	5392
991-245-9	245	X			X	5823	5402
check ✓ 991-245-E ?	245	X				?	?
991-265-1	265			X	X	6013	5497
991-265-1R	265				X	6013	5497

? check

Sample Number	Mine Level	Pol. Sect.	Pol. Slab	Pol. Plug	Geo-chem.
991-400-R1	400				X
991-0-2	0			X	X
991-365-Y	365	X			X
991-175-1	175	X			X
991-320-1	320	X			X
991-525-33	525	X			X
991-365-X	365	X			X
991-00-1		X			X
991-320-6	320	X			X
991-365-XR	365				X
991-400-R3	400	X			X
991-225-4	225	X			X
991-265-2	265	X		X	X
991-365-910	365	X			X
991-585-34	585	X		X	X
991-320-2	320	X			X
991-0-3B	0	X			X
991-245-11	245	X			X
991-320-8R	320				X
991-350-2	350	X			X
991-585-32	X				X
991-400-1R	400				X
991-0-3A	0				X
991-190-1	190				X
991-400-1	400			X(2)	X
991-G'	350	X			
245-E	245	X			
991-I'-C85	450	X			
430-5-65	430			X(2)	
430-4B-65	430			X	
991-A-C84 *	(dump)	X			
991-B'-C85	240	X			
991-C'-C85	310	X			
991-C-C85	310	X			
991-D'-C85	310	X			

X Uranerz

Orphan Samples

Outcrop	1-7	Book 4
Adit	1-9	Book 1
190	1	Book 3
225	1-6	Book 1
245	6-9, N-1	Book 1
290	1-11	Book 6
325	1-4	Book 3
350	20	Book 3
365	1-3	Book 1
	X, Y	Book 3
	11-16	Book 5
375	D-1	Book 6
400	R-1-R-4	Book 1
	1	Book 6
	11-16	Book 5
430	1	Book 1
	1A, 1B	Book 6
	2-20	Book 6
	1-6	Book 5

585	-1	Book 3
	2-5	Book 1

Borch 2 | Elench 175 - 5734' | adit
190 - 5722 12' | 59.09'
15

Borch 1 Geologic log 245 - 400

Sampler 365-1
-2
-3

Sampler 225 4
4b
5
6
1
2

sampler 365 1
2
3

Sampler 400 R-1
R-2
R-3
R-4

Sampler 430 - 1
Sampler 245 6
7
8
245 - 9
N-1

Sampler 585 - 3 ?
4
5
2

Sampler 0 - 1
adit 2 7
3 8
5 9
6

Book 3 350 - 20

585 -

365 X

365 Y

190 - 1

325 - 1

4

3

Book 4 Outing 0 - 1 0 - 7

0 - 2

0 - 3

0 4

0 - 5

0 - 6

Book 5

430 - 16 365 - 11

13

400 - 11 14

400 - 12 15

13 16

14 12

15

16

Book 6

430 1A		
1B		
2		
400 1 ✓		
375 D-1 ✓		
430 3	430 9	430-16
430 4A ✓	10	17
430 5 ✓	11	18
430 4B ✓	12	19
6	13	20
7	14	
8	15	

290-1	290-8
29B-3	-9
4	10
5	11
6	
7	

Sample Number	Mine Level	Pol. Sect.	Pol. Slab	Pol. Plug	Geo-chem.
991-G-C85	350	X			X
991-B-C85	240	X			X
991-K-C85	?	X			X
991-J-C85	outer annular ring	X			X
991-F-C85	310	X			X
991-D-C85	310	X			X
991-I-C85	450	X			X
991-E-C85	310	X			X
991-H-C85	450	X			X
991-W-C87	0	X			X
991-R-C87	100	X			X
991-S-C87	80	X			X
991-T-C87	0+15	X			X
991-U-C87	0	X			X
991-245-2	245				X
991-585-33B	585	X			X
991-245-9	245	X			X
991-320-4	320	X			X
991-320-8	320			X	X
991-245-4B	245				X
991-350-1	350	X			X
991-400-R4	400			X	X
991-365-3	365	X		X	X
991-365-1	365				X
991-245-4A	245				X
991-320-7	320	X			X
991-585-33A	585	X			X
991-350-365	350-365	X			X
991-245-11C	245	X			X
991-375-D-1	375	X			X
991-400-30	400	X		X	X
991-265-1	265			X	X
991-245-10	245	X			X
991-265-1R	265				X
991-350-21	350			X	X
991-245-5	245			X	X

WLC KJW VMG

Sample Number	Mine Level	Pol. Sect.	Pol. Slab	Pol. Plug	Geo-chem.
991-E'-C85	310	X			
991-F'-C85	310	X			
320	320	X			
991-DUMP2	(dump)	X		X	
245-4	245			X	
245-0-2	245			X	
585-3	585			X	
0-3A	0	X			
245-1	245	X			
365-2	365	X			
365-15	365	X			
400-2	400	X			
430-4A	430	X			
585-33	585	X			
400R2	400	X			
550-2	550			X(2)	
585-31-64	585			X	
1000/5557		X			
1190/5630		X			
1090/6630 ?		X			
760/5680		X			
900/5658		X			
1150/5480	420	X(2)			
8' ✓	400	X			
6' ✓	400	X			
5' ✓	190	X			
7 ✓	225	X			
11		X			
9			X		
5			X		
12			X		
4			X		
8 5960/5665	420		X		

8/14/95

Bill,

Here is the updated list of Orphan Mine samples -- one copy ordered by mine level and one by sample no. Due to the idiosyncrasies of alphanumeric sorting, the sample # list is not totally in order (1000 gets sorted before 11, for example) but we can tinker with that if needed for publication. Also returning your originals, just in case...

Regina

Orphan Mine Samples -- Ordered by Mine Level

Sample Number	Mine Level	Coordinates North	Coordinates East	Pol. Sect.	Pol. Slab	Pol. Plug	Geo-chem.
4		?	?		X		
5		?	?		X		
11		?	?		X		
991-K-C85	?	NA	NA	X			X
991-P-C86	?	NA	NA	X			
991-A-C84	(dump)	NA	NA	X			
991-DUMP1-C87	dump	NA	NA	X			
991-DUMP2-C87	(dump)	NA	NA	X			
991-J'-C85	outer annular ring	NA	NA	X			
991-J-C85	outer annular ring	NA	NA	X			X
991-0-2	0	?	?			X	X
991-0-3A	0	?	?	X			X
991-0-3B	0	?	?	X			X
991-00-1	0	?	?	X			X
991-U-C87	0	NA	NA	X			X
991-W-C87	0	NA	NA	X			X
991-T-C87	0-15	NA	NA				X
991-R-C87	080	NA	NA	X			X
991-S-C87	080	NA	NA	X			X
991-M-C86	100	NA	NA	X			
1000/5557	175	6000	5557	X			
991-175-1	175	6014	5524	X			X
991-Q-C86	175	5939	5581	X			
5'	190	5511	5972	X			
991-190-1	190	5942	5588				X
7	225	5322	5910	X			
991-225-4	225	6015	5562	X			X
991-B'-C85	240	NA	NA	X			
991-B-C85	240	NA	NA	X			X
991-245-0-2	245	5842	5430			X	
991-245-1	245	5920	5531	X			
991-245-10	245	5842	5420	X			X
991-245-11	245	?	?	X			X
991-245-11C	245	?	?	X			X
991-245-2	245	?	?				X
991-245-4	245	5792	5386			X	
991-245-4A	245	5792	5386				X
991-245-4B	245	5792	5386				X

Orphan Mine Samples -- Ordered by Mine Level

Sample Number	Mine Level	Coordinates		Pol. Sect.	Pol. Slab	Pol. Plug	Geo-chem.
		North	East				
991-245-5	245	5794	5392			X	X
991-245-9	245	5823	5402	X			X
991-245-E	245	?	?	X			
991-265-1	265	6013	5497			X	X
991-265-1R	265	6013	5497				X
991-265-2	265	5989	5536	X		X	X
900/5658	290	5900	5658	X			
991-C′-C85	310	NA	NA	X			
991-C-C85	310	NA	NA	X			
991-D′-C85	310	NA	NA	X			
991-D-C85	310	NA	NA	X			X
991-E′-C85	310	NA	NA	X			
991-E-C85	310	NA	NA	X			X
991-F′-C85	310	NA	NA	X			
991-F-C85	310	NA	NA	X			X
991-320	320	5938	5518	X			
991-320-1	320	5996	5709	X			X
991-320-2	320	5996	5709	X			X
991-320-4	320	5979	5701	X			X
991-320-6	320	5970	5697	X			X
991-320-7	320	6003	5695	X			X
991-320-8	320	5965	5686			X	X
991-320-8R	320	5965	5686				X
760/5680	350	5760	5680	X			
991-350-1	350	5743	5756	X			X
991-350-2	350	?	?	X			X
991-350-21	350	5770	5725			X	X
991-G′	350	NA	NA	X			
991-G-C85	350	NA	NA	X			X
991-350-365	350-365	6034	5470	X			X
991-365-1	365	6144	5524				X
991-365-15	365	?	?	X			
991-365-2	365	6130	5550	X			
991-365-3	365	6130	5550	X			X
991-365-Sta9-10	365	?	?	X			X
991-365-X	365	6069	5505	X			X
991-365-XR	365	6069	5505				X
991-365-Y	365	6069	5505	X			X
991-375-D-1	375	5834	5367	X			X

Orphan Mine Samples -- Ordered by Mine Level

Sample Number	Mine Level	Coordinates		Pol. Sect.	Pol. Slab	Pol. Plug	Geo-chem.
		North	East				
1090/6630	400	6090	5630	X			
12	400	?	?		X		
6'	400	6100	5629	X			
8'	400	6113	5632	X			
9	400	?	?		X		
991-400-1	400	6056	5567			X(2)	X
991-400-1R	400	6056	5567				X
991-400-30	400	?	?	X		X	X
991-400-R1	400	5622	6093				X
991-400-R2	400	5624	6095	X			
991-400-R3	400	5626	6097	X			X
991-400-R4	400	5625	6096			X	X
991-400-Z	400	?	?	X			
991-O'-C85	400	NA	NA	X			
991-O-C86	400	NA	NA	X			
1150/5480	420	6150	5480	X(2)			
8	420	5960	5665		X		
991-430-4A	430	6108	5617	X			
991-430-4B	430	6108	5617			X	
991-430-5	430	6108	5617			X(2)	
991-H'-C85	450	NA	NA	X			
991-H-C85	450	NA	NA	X			X
991-I'-C85	450	NA	NA	X			
991-I-C85	450	NA	NA	X			X
991-525-33	525	6045	5650	X			X
991-550-2	550	6138	5627			X(2)	
1190/5630	585	6190	5630	X			
991-585-3	585	6130	5700			X	
991-585-31	585	6127	5701			X	
991-585-32	585	6125	5702	X			X
991-585-33	585	6124	5703	X			X
991-585-33A	585	6124	5703	X			X
991-585-33B	585	6124	5703	X			X
991-585-34	585	?	?	X		X	X

? = can not locate sample location
NA = no location available

Sample Number	Mine Level	Coordinates North	Coordinates East	Pol. Sect.	Pol. Slab	Pol. Plug	Geo-chem.
1000/5557	175	6000	5557	X			
1090/6630	400	6090	5630	X			
11		?	?		X		
1150/5480	420	6150	5480	X(2)			
1190/5630	585	6190	5630	X			
12	400	?	?		X		
4		?	?		X		
5		?	?		X		
5'	190	5511	5972	X			
6'	400	6100	5629	X			
7	225	5322	5910	X			
760/5680	350	5760	5680	X			
8	420	5960	5665		X		
8'	400	6113	5632	X			
9	400	?	?		X		
900/5658	290	5900	5658	X			
991-0-2	0	?	?			X	X
991-0-3A	0	?	?	X			X
991-0-3B	0	?	?	X			X
991-00-1	0	?	?	X			X
991-175-1	175	6014	5524	X			X
991-190-1	190	5942	5588				X
991-225-4	225	6015	5562	X			X
991-245-0-2	245	5842	5430			X	
991-245-1	245	5920	5531	X			
991-245-10	245	5842	5420	X			X
991-245-11	245	?	?	X			X
991-245-11C	245	?	?	X			X
991-245-2	245	?	?				X
991-245-4	245	5792	5386			X	
991-245-4A	245	5792	5386				X
991-245-4B	245	5792	5386				X
991-245-5	245	5794	5392			X	X
991-245-9	245	5823	5402	X			X
991-245-E	245	?	?	X			
991-265-1	265	6013	5497			X	X
991-265-1R	265	6013	5497				X

Orphan Mine Samples

Sample Number	Mine Level	Coordinates		Pol. Sect.	Pol. Slab	Pol. Plug	Geo-chem.
		North	East				
991-265-2	265	5989	5536	X		X	X
991-320	320	5938	5518	X			
991-320-1	320	5996	5709	X			X
991-320-2	320	5996	5709	X			X
991-320-4	320	5979	5701	X			X
991-320-6	320	5970	5697	X			X
991-320-7	320	6003	5695	X			X
991-320-8	320	5965	5686			X	X
991-320-8R	320	5965	5686				X
991-350-1	350	5743	5756	X			X
991-350-2	350	?	?	X			X
991-350-21	350	5770	5725			X	X
991-350-365	350-365	6034	5470	X			X
991-365-1	365	6144	5524				X
991-365-15	365	?	?	X			
991-365-2	365	6130	5550	X			
991-365-3	365	6130	5550	X			X
991-365-Sta9-10	365	?	?	X			X
991-365-X	365	6069	5505	X			X
991-365-XR	365	6069	5505				X
991-365-Y	365	6069	5505	X			X
991-375-D-1	375	5834	5367	X			X
991-400-1	400	6056	5567			X(2)	X
991-400-1R	400	6056	5567				X
991-400-30	400	?	?	X		X	X
991-400-R1	400	5622	6093				X
991-400-R2	400	5624	6095	X			
991-400-R3	400	5626	6097	X			X
991-400-R4	400	5625	6096			X	X
991-400-Z	400	?	?	X			
991-430-4A	430	6108	5617	X			
991-430-4B	430	6108	5617			X	
991-430-5	430	6108	5617			X(2)	
991-525-33	525	6045	5650	X			X
991-550-2	550	6138	5627			X(2)	
991-585-3	585	6130	5700			X	
991-585-31	585	6127	5701			X	

Orphan Mine Samples

Sample Number	Mine Level	Coordinates North	Coordinates East	Pol. Sect.	Pol. Slab	Pol. Plug	Geo-chem.
991-585-32	585	6125	5702	X			X
991-585-33	585	6124	5703	X			X
991-585-33A	585	6124	5703	X			X
991-585-33B	585	6124	5703	X			X
991-585-34	585	?	?	X		X	X
991-A-C84	(dump)	NA	NA	X			
991-B'-C85	240	NA	NA	X			
991-B-C85	240	NA	NA	X			X
991-C'-C85	310	NA	NA	X			
991-C-C85	310	NA	NA	X			
991-D'-C85	310	NA	NA	X			
991-D-C85	310	NA	NA	X			X
991-DUMP1-C87	dump	NA	NA	X			
991-DUMP2-C87	(dump)	NA	NA	X			
991-E'-C85	310	NA	NA	X			
991-E-C85	310	NA	NA	X			X
991-F'-C85	310	NA	NA	X			
991-F-C85	310	NA	NA	X			X
991-G'	350	NA	NA	X			
991-G-C85	350	NA	NA	X			X
991-H'-C85	450	NA	NA	X			
991-H-C85	450	NA	NA	X			X
991-I'-C85	450	NA	NA	X			
991-I-C85	450	NA	NA	X			X
991-J'-C85	outer an-nular ring	NA	NA	X			
991-J-C85	outer an-nular ring	NA	NA	X			X
991-K-C85	?	NA	NA	X			X
991-M-C86	100	NA	NA	X			
991-O'-C85	400	NA	NA	X			
991-O-C86	400	NA	NA	X			
991-P-C86	?	NA	NA	X			
991-Q-C86	175	5939	5581	X			
991-R-C87	80	NA	NA	X			X
991-S-C87	80	NA	NA	X			X
991-T-C87	0-15	NA	NA				X
991-U-C87	0	NA	NA	X			X

Orphan Mine Samples

Sample Number	Mine Level	Coordinates		Pol. Sect.	Pol. Slab	Pol. Plug	Geo-chem.
		North	East				
991-W-C87	0	NA	NA	X			X

? = can not locate sample location
NA = no location available

400- 02
400- 1D
400- 3

ROCK SAMPLES

CHEM = chemical analysis
PS = polished sections from Bowles
TS = thin section

0-2	Very fine-grained. Non-calcareous sandstone with dark band of uraninite and copper minerals. Malachite impregnated. Uranium radioactive on sample = 5X. CHEM/PS
0-3A	Very fine-grained calcareous. Fine-grained pyrite impregnated. One sample has the hematite/uraninite association. Of three samples; one is calcareous and the other two are not. Radioactive on samples: 5 cm sample has 410 cps (64 bkg cps) and others have 510 cps (64 bkg cps) and 90 cps (64 bkg cps). TS/CHEM
0-3B	Very fine-grained non-calcareous sandstone. Yellowish gray. TS/CHEM
0-4	Slightly calcareous. Very fine-grained sandstone with black pods of copper(?) sulfides. Pale yellowish brown.
0-4a	Very fine-grained calcareous sandstone. Pale yellowish brown. Radioactive on sample: 73 cps (62 bkg cps).
175-1	Very fine-grained calcareous sandstone. Medium light gray. Radioactive on sample: 84 cps (52 bkg cps). TS/CHEM
190-1	Bag full of small barite chunks. Large barite crystals present. Minor malachite. Sphalerite may be present. CHEM
225-1	Very fine grained. Non-calcareous. Hematite impregnated sandstone. Brick red. (Description in book.)
225-4	Very fine-grained. Very slightly calcareous. Medium bluish gray with copper-rich nodules (chalcocite). Copper impregnated sandstone. (Description in book.) TS/CHEM
225-5	Very fine-grained calcareous sandstone with hematite-rich splotches that contain copper-rich areas. Minor malachite present. Grayish orange pink.
245-E	Very fine-grained calcareous sandstone impregnated with uraninite and copper metals. Ore sample. (E-raise.) TS
245-1	Mudstone. Calcareous. TS
245-2	Fine-grained sandstone. Calcareous with copper nodules. Grayish orange. Radioactive on sample = 3X. CHEM/PS
245-3	Limestone. Yellowish orange.
245-4A	Very fine grained calcareous sandstone. Abundant hematite and

uraninite. Classic hematite and uraninite relation. Abundant copper sulfides. Malachite. Radioactive on sample = HOT!! Probably greater than 1% uranium. CHEM/PS

245-4B	Very fine-grained calcareous sandstone. Hematite/uraninite association. Malachite and Azurite. Radioactive on sample: 540 cps (70 bkg cps). CHEM
245-4a	Light olive gray limestone.
245-4b	Very fine-grained. Slightly calcareous sandstone. Large calcite. Copper nodules. Copper impregnated. TS/CHEM
245-5	Very fine-grained. Non-calcareous. Malachite impregnated sandstone. Contains copper-rich nodules and lenses. Azurite. Radioactive on sample: 4400 cps (100 bkg cps) = HOT!! CHEM/PS
245-6	Very fine-grained calcareous sandstone. Hematite/uraninite association.
245-8	Very fine-grained. Very calcareous sandstone. Light Brown.
245-9	Light olive grey sandstone. TS/CHEM
245-10	Very fine-grained calcareous sandstone. Radioactive: 62 cps (50 bkg cps). Grutt locality. CHEM
245-10	Very fine-grained calcareous sandstone. TS/CHEM
245-11	Very fine-grained. Highly calcareous sandstone. Grayish orange with grey band. Probably uraninite impregnation of sandstone. Deep orange band. Probably limonite-rich. Radioactive on sample: 120 cps (54 bkg cps). TS/CHEM
245-11a	Very fine-grained. Very calcareous sandstone. Yellowish gray (Located on map.)
245-11b	Limestone. Grayish pink. (Located on map.)
245-11c	Very fine-grained calcareous sandstone. Grayish red. (Unaltered Supai Annular Ring: Located on map.) TS/CHEM
265-1	Chalcocite, malachite.
265-1	Very fine-grained. Calcareous sandstone with abundant malachite. Contains copper-rich nodules. Copper minerals form a cement within the sandstone around the nodule. Grayish orange. Copper carbonate (B stope) covellite. CHEM/PS
265-2	Very fine-grained. Calcareous. Pyrite impregnated sandstone. Sample has desiccation crack. CHEM/PS

320	Very fine-grained slightly calcareous sandstone. Hematite/uraninite association. Radioactive on sample: 140 cps (62 bkg cps). TS CHEM
320-1	Fine-grained sandstone. Very slightly calcareous. 1/2 cm crystals of galena. Light brown. TS/CHEM
320-2	Very fine-grained sandstone. Slightly calcareous. Pale yellowish brown. Radioactive on sample: 120 cps (70 bkg cps). CHEM/TS
320-3	Fine-grained calcareous sandstone. Grayish yellow green. (Same as 320-4.)
320-4	Fine-grained calcareous sandstone. Greenish gray. TS/CHEM
320-5	Fine-grained calcareous sandstone. Light olive gray. Malachite standing on fractures. (Same as 320-4.)
320-6	Fine-grained calcareous sandstone. Greenish gray (same look as 320-4). Radioactive on sample: 100 cps (70 bkg cps). TS/CHEM
320-7	Fine-grained. Slightly calcareous. Yellowish gray. Radioactive on sample: 91 cps (62 bkg cps). TS/CHEM
320-8	Medium fine-grained calcareous sandstone impregnated by abundant metals (copper and uranium). Medium dark gray. Radioactive on sample: 410 cps (70 bkg cps). CHEM/PS
350-1	Fine-grained calcareous sandstone. Radioactive on sample: 320 cps (60 bkg cps). TS/CHEM
350-2	Very fine-grained slightly calcareous sandstone with some hematite/malachite bands. Pinkish gray. TS/CHEM
350-21	Medium fine-grained. Non-calcareous. Copper (Mo?) impregnated sandstone. Dark gray. CHEM/PS
350-365	Very fine-grained non-calcareous sandstone. Medium olive gray. TS/CHEM
365-X	Calcareous. Light gray and light olive gray. Radioactive on sample: 150 cps (62 bkg cps). TS/CHEM
365-Y	Fine-grained non-calcareous sandstone with 2 cm reduction spots with limonite halos. Blades of iron-stained barite(?). Galena. TS/CHEM
365-1	Very fine-grained non-calcareous sandstone. Grayish orange. Radioactive on sample : 100 cps (62 bkg cps). CHEM
365-2	Medium fine-grained non-calcareous sandstone. Abundant limonite staining. Grayish orange. Radioactive on sample: 97 cps (70 bkg cps).

365-2	Very fine-grained sandstone. Slightly calcareous. Alternating 1 cm red hematite stained bands with 1/2 cm bleached bands containing cores of dark copper (uranium) minerals. "Zebra" rock. Yellowish gray. Radioactive on sample: 125 cps (64 bkg cps) TS/CHEM
365-3	Non-calcareous. Fine and medium sand grains in sandstone. Appears to be some medium-grained coconino sand mixed with fine-grained sand. A band of fine-grained sand impregnated with iron and/or copper. Medium olive gray. TS/CHEM
? 365-sta. 10	Fine-grained. Very very slightly calcareous. Copper bearing 9-sandstone. Grayish pink. TS/CHEM
365-11	Very very fine-grained calcareous vuggy sandstone. Pale yellowish brown.
365-15	Very very fine-grained slightly calcareous. Medium olive gray. TS
375-D-1	Very fine-grained slightly calcareous sandstone with calcite veins. Large crystals of calcite. Pale yellowish brown. TS/CHEM/FI
400-1	Fine-grained slightly calcareous sandstone. Pyrite, chalcopyrite, and galena present. Grayish orange.
400-R1	Non-calcareous. Very fine-grained impregnated with copper, uraninite, and cobalt. Radioactive on sample: 78 cps (62 bkg cps). CHEM
400-R2	Very fine-grained non-calcareous sandstone with pyrite nodules. Grayish orange. TS
400-R3	Very fine-grained non-calcareous sandstone. Desiccation cracks. Pyrite impregnated. TS/CHEM
400-R4	Very fine-grained. Very very slightly calcareous. Copper, uraninite, and cobalt impregnated sandstone. Light olive gray. Radioactive on sample: 78 cps (62 bkg cps). CHEM/PS
400-Z	Very fine-grained calcareous sandstone with lense of calcite incased in 1/2 cm bleached band of fine-grained sandstone. Bleached reduction spot present that is very very slightly calcareous. Grayish red. TS
400-1	Dickite, koalinite.
400-1	Wulfenite.
400-1	Very fine-grained slightly calcareous sandstone. Veins and nodules of pyrite. Crystal nodules are 1/4 cm across. Pyrite disseminated from sandstone. Light olive gray. CHEM/PS
400-3	Very fine-grained. Calcareous pyrite impregnated sandstone.

400-2

400-30	Non-calcareous fine-grained sandstone impregnated with pyrite. Massive pyrite along fracture and nodules. Olive gray. TS/CHEM/PS
430-30	Non-calcareous. Pyrite nodules. Fine-grained barite. Grayish orange. TS/CHEM
430	Very fine-grained non-calcareous mudstone sample. Pale yellowish brown.
430-1	Very fine-grained. Calcareous. Grayish orange pink.
430-4a	Very fine-grained slightly calcareous sandstone with band of uraninite and copper(?) impregnated minerals. Grayish orange. Radioactive on sample: 80 cps (62 bkg cps). TS
430-4B	PS
430 -5	(Light colored sample.) PS
430-5	(Dark colored sample.) PS
525-33	Fine-grained. Very Very slightly calcareous. Copper sulfide/uraninite impregnated sandstone. Radioactive on sample: 78 cps (54 bkg cps). TS/CHEM
550-2	Unknown. PS
550-2(a?)	Breccia with very fine-grained calcareous sandy matrix. Heterogenous. Some clasts pyrite.
550-2a-1	Torbernite.
550-2a-3	Calcite.
550-2a-4	Bornite.
585-2	Limestone.
585-3	Marcasite, quartz
585-3	Very fine-grained. Non-calcareous sandstone with copper sulfides (uraninite??) Pyrite concentration. PS
585-5	Very fine-grained. Very very slight calcareous sandstone. Grayish orange pink.
585-30	Hematitic dirt.
585-31	PS
585-32	Very fine-grained slightly calcareous sandstone. Hematite/uraninite association. Abundant copper sulfide. Malachite. Azurite.

	Radioactive on sample: 480 cps (54 bkg cps). TS/CHEM
585-32	Same sample as above but unmineralized. Fine-grained non-calcareous sandstone. Yellowish gray. TS/CHEM
585-33a	Very fine-grained. Non-calcareous. Grayish orange pink. TS/CHEM
585-33b	Very fine-grained non-calcareous sandstone. Banding present. Radioactive on sample: 75 cps (54 bkg cps). TS/CHEM
585-34	Non-calcareous. Fine-grained hematite/limonite. Pyrite impregnated sandstone. Radioactive on sample: 82 cps (54 bkg cps). TS/CHEM/PS
Filter Paper Sample	(found with viles)
Orphan Mine (Location Unknown) 00-1	Very fine-grained calcareous sandstone. Abundant calcite. Looks brecciated?? Light gray and grayish orange. Radioactive on sample: 410 cps (62 bkg cps). TS CHEM
Redenour 2	Carnotite